Calhoun
Institutional Archive of the Naval Postgraduate School

Calhoun: The NPS Institutional Archive

DSpace Repository

Theses and Dissertations | 1. Thesis and Dissertation Collection, all items

1991-12

Orbital maintenance of endoatmospheric low earth-orbiting satellites

Pauls, David D.

Monterey, California. Naval Postgraduate School

http://hdl.handle.net/10945/26679

This publication is a work of the U.S. Government as defined in Title 17, United States Code, Section 101. Copyright protection is not available for this work in the United States.

Downloaded from NPS Archive: Calhoun

DUDLEY KNOX LIBRARY

Calhoun is the Naval Postgraduate School's public access digital repository for research materials and institutional publications created by the NPS community. Calhoun is named for Professor of Mathematics Guy K. Calhoun, NPS's first appointed -- and published -- scholarly author.

Dudley Knox Library / Naval Postgraduate School
411 Dyer Road / 1 University Circle
Monterey, California USA 93943

http://www.nps.edu/library

DUDLEY KNOX LIBRARY
NAVAL POSTGRADUATE SCHOOL
MONTEREY CA 93943-5101

Approved for public release: Distribution is unlimited

Orbital Maintenance of Endoatmospheric Low Earth-Orbiting Satellites

by

David D. Pauls
Lieutenant, United States Navy
B.A., Physics, Eastern Washington University, 1982

Submitted in partial fulfillment of the
requirements for the degree of

MASTER OF SCIENCE
IN ASTRONAUTICAL ENGINEERING

from the

NAVAL POSTGRADUATE SCHOOL

DECEMBER 1991

Unclassified

CURITY CLASSIFICATION OF THIS PAGE

REPORT DOCUMENTATION PAGE

Form Approved
OMB No 0704-0188

a. REPORT SECURITY CLASSIFICATION
Unclassified

1b. RESTRICTIVE MARKINGS

a. SECURITY CLASSIFICATION AUTHORITY

3. DISTRIBUTION/AVAILABILITY OF REPORT
Approved for public release: Distribution is unlimited

. DECLASSIFICATION/DOWNGRADING SCHEDULE

PERFORMING ORGANIZATION REPORT NUMBER(S)

5. MONITORING ORGANIZATION REPORT NUMBER(S)

. NAME OF PERFORMING ORGANIZATION
Naval Postgraduate School

6b. OFFICE SYMBOL *(If applicable)*
AA

7a. NAME OF MONITORING ORGANIZATION
Naval Postgraduate School

. ADDRESS *(City, State and ZIP Code)*
Monterey, CA 93943-5000

7b. ADDRESS *(City, State, and ZIP Code)*
Monterey, CA 93943-5000

. NAME OF FUNDING/SPONSORING ORGANIZATION

8b. OFFICE SYMBOL *(If applicable)*

9. PROCUREMENT INSTRUMENT IDENTIFICATION NUMBER

. ADDRESS *(City, State, and ZIP Code)*

10. SOURCE OF FUNDING NUMBER

PROGRAM ELEMENT NO.	PROJECT NO.	TASK NO.	WORK UNIT ACCESSION NO

. TITLE *(Include Security Classification)*
ORBITAL MAINTENANCE OF ENDOATMOSPHERIC LOW EARTH-ORBITING SATELLITES

. PERSONAL AUTHORS
DAVID D. PAULS

a. TYPE OF REPORT
Master's Thesis

13b. TIME COVERED
FROM_______ TO_______

14. DATE OF REPORT *(Year, Month, Day)*
DECEMBER 1991

15. PAGE COUNT
71

. SUPPLEMENTARY NOTATION
The views expressed are those of the author and do not reflect the official policy or position of the Department of Defense or the U.S. Government

. COSATI CODES

ELD	GROUP	SUB-GROUP

18. SUBJECT TERMS *(Continue on reverse if necessary and identify by block numbers)*
orbits, satellites, low-Earth orbiting satellites, fuel-minimization

. ABSTRACT *(Continue on reverse if necessary and identify by block numbers)*

The optimization of spacecraft trajectories in vacuum has received extensive consideration ince the inception of space flight, yet, the effects of atmosphere have been largely neglected. The dvent of low Earth-orbiting, large satellites and platforms necessitates that atmosphere be included n the optimization process. A practical means of studying this topic is as a problem in minimum-fuel rbital maintenance. Optimal control theory advances the notion that orbital maintenance is optimized hrough periodic thrusting as opposed to forcing Keplarian motion by nullifying the effects of drag ith thrust. Further, this must be optimized by primer vectoring. This thesis examined the efficiency f a simple method of orbital maintenance using fixed-angle transverse thrusting. Results show that or the purpose of fuel-minimization, the width of the radial band in which the satellite is to be aintained, is dependent upon thruster size. In nearly all cases, a thrust-angle of 70 degrees aximized the fuel saved. This thesis shows that fixed-angle transverse thrusting does not improve n forced Keplarian motion and hence thrust vectoring must be optimized.

DISTRIBUTION/AVAILABILITY OF ABSTRACT
XX UNCLASSIFIED/UNLIMITED __ SAME AS RPT __ DTIC USERS

21. ABSTRACT SECURITY CLASSIFICATION
unclassified

a. NAME OF RESPONSIBLE INDIVIDUAL
I.M. Ross

22b. TELEPHONE *(Include Area Code)*
(408) 646-2716

22c. OFFICE SYMBOL
AA/Ro

Form 1473, JUN 86

Previous editions are obsolete.

S/N 0102-LF-014-6603

SECURITY CLASSIFICATION OF THIS PAGE
Unclassified

NAVAL POSTGRADUATE SCHOOL
Monterey, California

THESIS

ORBITAL MAINTENANCE OF ENDOATMOSPHERIC LOW EARTH-ORBITING SATELLITES

by

David D. Pauls

DECEMBER 1991

Thesis Advisor: I.M. Ross

Approved for public release: Distribution is unlimited

ABSTRACT

The optimization of spacecraft trajectories in vacuum has received extensive consideration since the inception of space flight, yet, the effects of atmosphere have been largely neglected. The advent of low Earth-orbiting, large satellites and platforms necessitates that atmosphere be included in the optimization process. A practical means of studying this topic is as a problem in minimum-fuel orbital maintenance. Optimal control theory advances the notion that orbital maintenance is optimized through periodic thrusting as opposed to forcing Keplarian motion by nullifying the effects of drag with thrust. Further, this must be optimized by primer vectoring. This thesis examined the efficiency of a simple method of orbital maintenance using fixed-angle transverse thrusting. Results show that for the purpose of fuel-minimization, the width of the radial band in which the satellite is to be maintained, is dependent upon thruster size. In nearly all cases, a thrust-angle of 70 degrees maximized the fuel saved. This thesis shows that fixed-angle transverse thrusting does not improve on forced Keplarian motion and hence thrust vectoring must be optimized.

The
P[illegible]
c.1

TABLE OF CONTENTS

I. INTRODUCTION 1
II. GENERAL FORMULATION OF THE PROBLEM 4
III. SIMPLIFIED PARAMETRIC FORMULATION 8
  A. DEVELOPMENT OF THE EQUATIONS OF MOTION . . . 8
  B. DETERMINATION OF THE CONTROL VARIABLE 10
IV. DEVELOPMENT AND TESTING OF THE COMPUTER MODEL . 12
  A. COMPUTER PROGRAM DEVELOPMENT 12
  B. PROGRAM VALIDATION 13
    1. Development of a Rule of Thumb 14
    2. Development of a Control Law 15
    3. Control Law design 16
      a. Approximate method 16
      b. Direct method 20
V. ANALYSIS AND RESULTS 22
  A. USE OF A CONSTANT DENSITY MODEL 22
  B. USE OF AN EXPONENTIAL ATMOSPHERIC MODEL . . . 23
    1. Comparison with a Forced-Keplarian Model 24
    2. Further Testing 25
      a. Constant Thrust, Varied Specific Impulse 25
      b. Constant Specific Impulse, Varied Thrust 27
    3. Final Tests 28
      a. Case 1: Thrusters Fire 20 km Below R_0 28
      b. Case 2: Thrusters Fire 30 km Below R_0 30
      c. Case 3: Thrusters Fire 40 km Below R_0 31
  C. SUMMARY OF RESULTS 32
VI. CONCLUSIONS AND RECOMMENDATIONS 33

NAVAL POSTGRADUATE SCHOOL
MONTEREY CA 93943-5101

APPENDIX A 36
APPENDIX B 43
APPENDIX C 45
APPENDIX D 47
APPENDIX E 50
APPENDIX F 53
APPENDIX G 56
APPENDIX H 57
APPENDIX I 58
LIST OF REFERENCES 61
INITIAL DISTRIBUTION LIST 62

LIST OF FIGURES

Figure 1 Graphical Representation of Coordinate System 9

Figure 2 Path Travelled By A Spacecraft Between Two Orbits 16

NOMENCLATURE

a_r	radial acceleration
a_{tr}	transverse acceleration
a	semi-major axis of an ellipse
C	negative reciprocal of thruster exhaust velocity
C_D	coefficient of drag
D	magnitude of drag
D_r	radial component of drag
D_{tr}	transverse component of drag
E	total energy
F_r	external forces in radial direction
F_{tr}	external forces in transverse direction
g_o	gravitational acceleration at sea level
H	Pontryagin's H-function
I_{sp}	specific impulse
$\underline{\ell}$	unit vector in direction of thrust
m	spacecraft mass
$\underline{r}$	position vector
r	radius
r_{max}	maximum radius
r_{min}	minimum radius
R_o	initial radius
R_f	final radius
S	path travelled by spacecraft
S1	initial position of spacecraft
S2	final position of spacecraft
S_{ref}	aerodynamic reference surface of vehicle
$\vec{T}$	thrust vector
T_{max}	magnitude of thrust
T_r	radial component of thrust
T_{tr}	transverse component of thrust
t	time
t_o	initial time

t_f	final time
v	velocity
$\underline{v}$	velocity vector
v_r	radial component of velocity
v_{tr}	transverse component of velocity
α	thrust angle
β	exponential density scale factor
ΔE	change in total energy
ΔR	radius at which periodic thrusting is commenced
Δt	change in time
$\mathcal{E}$	specific energy
θ	orbital coordinate used to define spacecraft position
λ	Lagrange multiplier
λ_m	mass costate
$\underline{\lambda}_v$	velocity costate vector
$\underline{\lambda}_r$	radius costate vector
μ	gravitational constant
ρ	atmospheric density
ρ_o	atmospheric reference density

I. INTRODUCTION

In 1963, D.F. Lawden, in his monograph [Ref. 1], laid the foundation for what has become a highly sophisticated subdiscipline of astrodynamics, optimization of space trajectories. In 1979, Marec [Ref. 2] provided a more comprehensive treatment of the subject in his text on optimal space trajectories. Examination of the optimization of spacecraft trajectories has been treated by many authors in manners similar to these two great works, yet, until recently, the study of atmospheric effects upon these trajectories was largely neglected. Research and development of hypervelocity vehicles have kindled interest in this area, through which study, other areas of interest have emerged.

One such area is the effect of aerodynamic force on non-lifting, or, blunt bodies. First addressed by Ross and Melton [Ref. 3], this subject is of particular interest for two reasons. First, atmospheric effects on low-Earth orbiting (LEO) satellites are of obvious interest and second, as stated in their paper [Ref. 3:p. 2], better understanding of this phenomenon could provide deeper insight into the more complicated topic of lifting bodies in the upper atmosphere.

Much work has been accomplished in this area pertaining to accurate prediction of satellite orbits [Ref. 4, 5]. The focus on atmospheric effects as they pertain to the specific problem of minimum-fuel orbital transfers, however, is unique to [Ref. 3] and the follow-on work described here. The particular problem of orbital maintenance can provide insight into the more general, and complex problem of orbital transfer.

Historically, orbital transfers (coplanar) have been accomplished as either, two, or, three-impulse maneuvers [Ref. 6:pp 78-88]. The problem of orbital transfer is approached as a minimization of energy required to move a satellite from orbit A to orbit B, or, equivalently, a minimization of the characteristic velocity. A satellite that has descended from an initial orbit due to a disturbing force such as drag, and which must be returned to its initial orbit can be approached as a problem requiring an orbital transfer. Orbital transfers such as this are optimally performed by two-impulse transfers, such as a Hohman transfer. Large orbital transfers ($r_a>11.8r_p$) are optimized with three-impulse maneuvers [Ref. 6:p 87]. As low-Earth orbits become more frequently utilized, deeper understanding of the effects of drag must be achieved in order that orbits, propulsion systems and costs are optimized. This is particularly applicable for large satellites, such as the proposed space station, that must remain in low orbits for extended periods of time.

Additionally, more complex areas of study, such as that of lifting bodies in the upper atmosphere, could benefit from the insights gained through a deeper understanding of atmospheric effects on non-lifting bodies.

Research on the atmospheric effects on low-Earth orbiting spacecraft is sure to receive much attention in the future. The benefits to existing and future systems, while extensive, remain relatively unexplored and demand the attention of the aerospace industry.

II. GENERAL FORMULATION OF THE PROBLEM

Optimization of orbital transfers is a subject that has achieved a high degree of sophistication and many elegant solutions exist [Ref. 1, 2]. However, the specific treatment of non-lifting bodies is in the initial stages of development. The increasing number of low Earth orbiting satellites requires that a study of atmospheric effects on orbital trajectories be conducted. In this thesis, the problem of minimum fuel orbital maintenance is considered. Two methods are examined by which orbital maintenance may be performed.

One method is to counter drag with thrust. In this forced Keplarian motion, the reaction control system would thrust continuously for the duration of the satellite's lifetime with magnitude and direction equal and opposite to drag. The second scheme considered here, utilizes periodic transverse thrusting, or, non-Keplarian motion to correct for perturbations due to drag. The question to be answered is whether or not optimal non-Keplarian trajectories are superior to forced-Keplarian trajectories.

Let the problem be defined as maintaining an orbital deviation within a specified radial band $r_{min} \leq r \leq r_{max}$. Is forced-Keplarian orbital maintenance, i.e., exactly countering aerodynamic forces with thrust, superior to non-Keplarian orbital maintenance, i.e., allowing the orbit to decay to a certain point, then reboosting to a point above the desired altitude. While maintaining the spacecraft within the specified radial band? The study performed by Ross and Melton [Ref. 3:p. 4] suggests that forced-Keplarian motion is not optimal and that thrust vectoring must be considered if an optimal solution is to be obtained.

This thesis addresses an additional question, can orbital maintenance be optimized if thrusters are fired at a fixed angle to the local horizon and if so, what is the angle or, preferably, range of angles that achieve optimality?

Ross and Melton [Ref. 3] develop their theory through the methods of optimal control theory. It is proposed here that, while ideally accomplished in that manner, satisfactory and enlightening results may be obtained through the use of relatively unsophisticated mathematics and the aid of computer modelling techniques. To exemplify this statement, let us examine the mathematical development in Ross [Ref. 3: pp. 1-3]. Drag is given by

$$\underline{D} = -\frac{1}{2}\rho(\underline{r}) S_{ref} C_D v \underline{V} \tag{1}$$

where $\rho(r)$ is atmospheric density, S_{ref} is the reference surface area of the spacecraft upon which the aerodynamic forces act, C_D is spacecraft's coefficient of drag and v is its velocity. The equations of motion can be written as

$$\underline{\dot{r}} = \underline{v} \tag{2}$$

$$\dot{\underline{V}} = -\frac{\mu}{r^3}\underline{r} - \left(\frac{S_{ref}C_D}{2}\right)\frac{\rho V}{m}\underline{V} + \frac{T_{max}}{m}\underline{1} \tag{3}$$

$$\dot{m} = CT_{max}; \qquad \left(C = -\frac{1}{I_{sp}g_0}\right) \tag{4}$$

Applying the principles of Pontryagin, the Hamiltonian is given by

$$H = \underline{\lambda_r V} - \left(\frac{S_{ref}C_D}{2}\right)\frac{\rho V}{m}\underline{\lambda_v V} - \frac{\mu}{r^3}\underline{\lambda_v r} + \frac{T_{max}}{m}\underline{\lambda_v 1} + \lambda_m C T_{max} \tag{5}$$

The costates are then written as

$$-\underline{\lambda_r} = \frac{\partial H}{\partial \underline{r}} = -\left(\frac{S_{ref}C_D}{2}\right)\underline{\lambda_v V}\left(\frac{V}{m}\right)\left(\frac{\partial \rho}{\partial \underline{r}}\right) - \frac{\mu}{r^3}\underline{\lambda_v} + \mu\underline{\lambda_v r}\left(\frac{3}{r^5}\right)\underline{r} \tag{6}$$

$$-\underline{\lambda_v} = \frac{\partial H}{\partial \underline{V}} = \underline{\lambda_r} - \left(\frac{S_{ref}C_D}{2}\right)\frac{\rho V}{m}\underline{\lambda_v} - \left(\frac{S_{ref}C_D}{s}\right)\frac{\rho}{m}\underline{\lambda_v V}\left(\frac{\underline{V}}{V}\right) \tag{7}$$

$$-\lambda_m = \frac{\partial H}{\partial m} = \left(\frac{S_{ref}C_D}{2}\right)\rho V\underline{\lambda_v V}\left(\frac{1}{m^2}\right) + T_{max}\underline{\lambda_v 1}\left(\frac{1}{m}\right) \tag{8}$$

A closed form solution to these equations does not exist and only after initial and boundary conditions have been determined may the solution be obtained through numerical integration. This is a cumbersome method for determining the optimal direction of thruster firing. In this thesis, we look into the possibility of a constant vectoring scheme that may result in nearly identical performance.

A computer generated model will strive to maintain spacecraft trajectory within ±1.5 kilometers of the injection altitude utilizing a periodic fixed angle transverse thrusting control scheme whose direction is maintained at a fixed angle relative to the local horizon. The propellant consumed will then be compared to that of the same satellite employing a control law that sets thrust equal to drag at every point within the orbit.

III. SIMPLIFIED PARAMETRIC FORMULATION

A method less elegant than optimal control theory, but nonetheless valid, is that of parametric variation. The equations of motion are developed for the satellite's orbital trajectory and certain parameters varied to achieve "optimal" control of orbital variations.

A. DEVELOPMENT OF THE EQUATIONS OF MOTION

For the purpose of building a solid foundation, certain simplifying assumptions are made. Orbital motion is assumed to be coplanar, the initial spacecraft orbit is assumed to be circular and since the spacecraft is a non-lifting (blunt) body, drag is the net aerodynamic force acting upon it.

The equations of motion for this two-body system can be written as

$$a_r = \sum \frac{F_r}{m} \tag{9}$$

$$a_{tr} = \sum \frac{F_{tr}}{m} \tag{10}$$

where a_r is the radial acceleration of the spacecraft, a_{tr} is its transverse acceleration, F_r is the sum of the external forces in the radial direction, F_{tr} is the sum of the external forces in the transverse direction and m is spacecraft mass.

The external forces acting on the spacecraft are the gravitational field, aerodynamic forces and thrust. Figure 1 illustrates the coordinate system and the net forces.

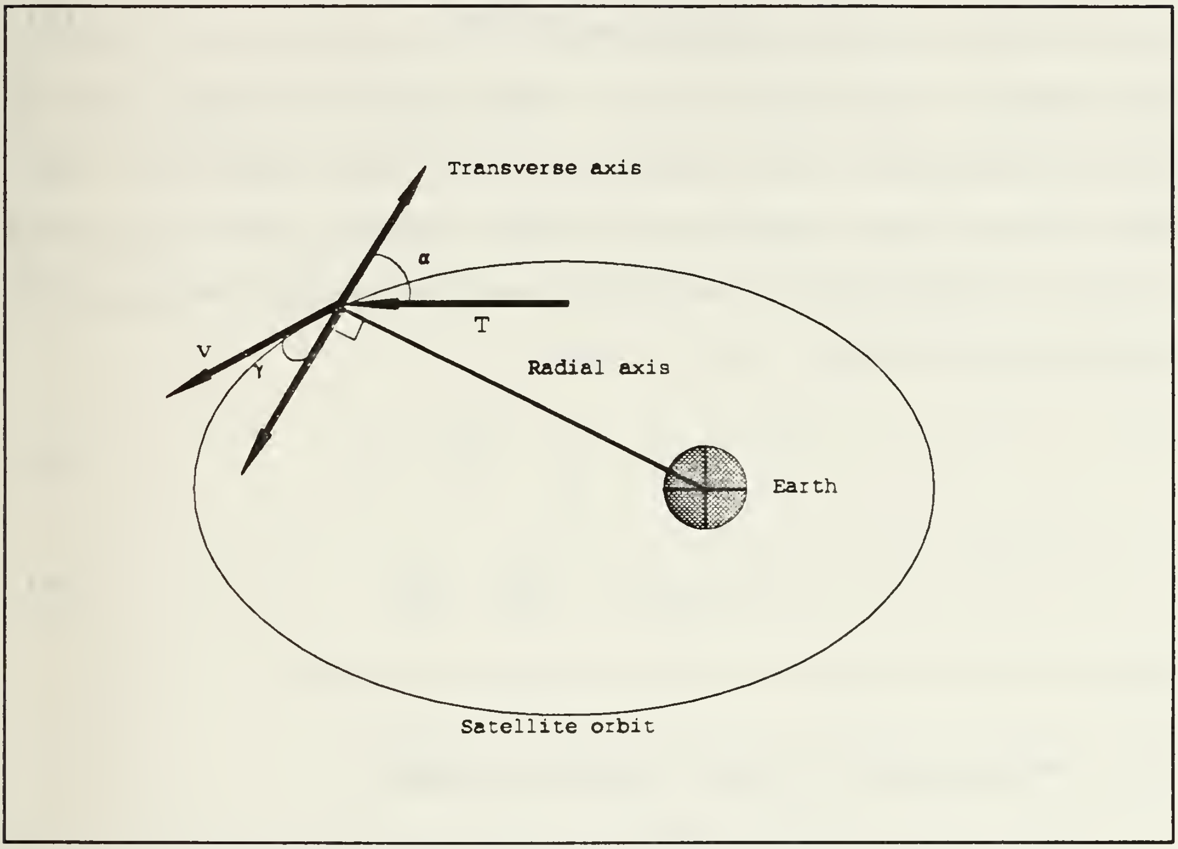

Figure 1 Graphical Representation of Coordinate System

Referring to Figure 1, it is clearly seen that the components for drag are given by

$$D_r = -D\sin(\gamma) \tag{11}$$

$$D_{tr} = -D\cos(\gamma) \tag{12}$$

Likewise, thrust is written as

$$T_r = T_{\max} \cos(\alpha) \tag{13}$$

$$T_{tr} = T_{\max} \sin(\alpha) \tag{14}$$

The angle γ is the flight path angle, defined by the intersection of the velocity vector and the transverse axis. The angle α is called the thrust angle, defined by the intersection of the thrust vector and the transverse axis. The equations of motion, then, become

$$\ddot{r} - \theta^2 r = -\frac{\mu}{r^2} - \frac{D_r}{m} + \frac{T_r}{m} \tag{15}$$

$$\theta r + 2\theta\dot{r} = -\frac{D_{tr}}{m} + \frac{T_{tr}}{m} \tag{16}$$

where μ is the Earth's gravitational constant.

B. DETERMINATION OF THE CONTROL VARIABLE

Following the development of the previous chapter, it is desirable to maintain the spacecraft within a radial band of a predetermined width. This may be accomplished by directly controlling either radius or eccentricity. Radius is the control variable of choice for a number of reasons: it is found directly from integration of the equations of motion, changes are easily visualized and radius control provides indirect control of the eccentricity. It is clear that by varying the thrust, control of satellite radius is possible. Examination of the thrust equations (Equations 13 and 14), presents two methods by which thrust may vary, changes of amplitude or change in the direction of the thrust vector.

The following chapter presents a method by which radial deviation is controlled through variation of the thrust angle and then tested by varying the thrust magnitude. A computer model is developed that simulates the trajectory of a spacecraft, graphically demonstrating the effects imposed on it through variation of the direction of the thrust.

IV. DEVELOPMENT AND TESTING OF THE COMPUTER MODEL

A. COMPUTER PROGRAM DEVELOPMENT

As indicated in the previous chapter, a computer program is developed to simulate spacecraft orbital trajectories and is included in Appendix A. The program is written in the fortran language and employs a fourth-order Runge-Kutta numerical integration routine to integrate the equations of motion. The program consists of six sections, the main program and five subroutines. The main program controls input and output while the subroutines provide various other functions necessary for accurate simulation of orbital trajectories.

The first subroutine calculates drag experienced by the spacecraft. Initially, a model incorporating constant atmospheric density is used. This facilitates verification of the program, after which, an exponential density model is used. It is acknowledged that more accurate atmospheric density models exist, however, the exponential model provides satisfactory accuracy over the range of travel experienced by the satellite (± 1.5 kilometers from initial orbit R_0) as controlled by the simulation. The second subroutine contains the equations of motion governing the spacecraft's orbital trajectory. To facilitate handling, the equations were broken into parts. Solving Equations (15) and (16) for acceleration, it is seen that the right-hand side of the radial equation has four components and the angular equation has three. These components are labeled A, B, C, and E for the radial equation and P, Q and S for the equation governing angular motion. The third subroutine contains the fourth-order Runge-Kutta numerical integration routine used to integrate the equations of motion. The next subroutine calculates the parameters of the satellite's osculating orbit. The last subroutine contains the control law governing the activation and deactivation of the thrusters responsible for the periodic maintenance of the satellite's orbit.

The following parameters define the specifications around which the computer model was developed.

- Spacecraft mass = 20,000 kg.
- Spacecraft frontal area (S_{ref}) = 60 m^2.
- Coefficient of drag (C_D) = 2.2.
- Altitude of spacecraft's orbit (R_0) = 260 km.
- Atmospheric density at R_0 (ρ) = 8.3130×10^{-11} kg/m^3.

B. PROGRAM VALIDATION

Program development proceeded in stages, with each stage requiring validation prior to beginning the next. Initially, all external forces except gravitation were neglected. Clearly, radius, speed, angular momentum and specific energy must remain constant for the program to be considered valid.

Having accomplished that elementary stage, phase two introduced drag (Equation (1)). Taking into account the fact that aerodynamic forces acting on a spacecraft are very small, and consequently, the time required for significant changes to occur, very large, atmospheric density was increased by approximately three orders of magnitude in order to reduce computer run time.

Initially verifying that radius continually decreased, the accuracy was tested by comparing the difference in altitude per orbit calculated by the program to that calculated manually by simplified equations. This is accomplished through the use of a "rule-of-thumb" and is developed in the following section.

1. Development of a Rule of Thumb

Work done by drag is a function of the path travelled by the spacecraft. Therefore, the amount of work done corresponds to the change in energy of the spacecraft, which is given by

$$Work\ done = \Delta E = Drag \times 2\pi r \tag{17}$$

Spacecraft specific energy is given by

$$\mathscr{E} = \frac{v^2}{2} - \frac{\mu}{r} = -\frac{\mu}{2a} \tag{18}$$

Total energy E is equal to the specific energy multiplied by spacecraft mass. Assuming that the spacecraft is in a circular orbit, the semi-major axis a is equal to the radius r.

Performing this substitution then differentiating both sides of the equation while holding mass constant yields

$$dE = \frac{\mu m}{2r^2}\,dr \tag{19}$$

Setting Equations (17) and (19) equal to each other and solving for the change in radius yields

$$\Delta r = \frac{4\pi r^3 D}{\mu m} \tag{20}$$

Equation (20) is the decrease in radius per orbit of the spacecraft due to drag. Despite inaccuracies resulting from the simplifying assumptions, this rule of thumb is accurate to within a few percent. The difference in spacecraft radius calculated by the computer program matched that of the thumb rule within a few percent thereby validating the model through this point in its development. Phase three introduced thrust while setting drag equal to zero. Clearly, any results other than steadily increasing radius, angular momentum, and specific energy would have been cause for program invalidation.

2. Development of a Control Law

The purpose of the control law is to maintain satellite radius within a prespecified bandwidth. By monitoring certain variables, activation and deactivation of station keeping thrusters can be determined. Keeping the control law simple in order that computer memory and run time related to station keeping be kept to a minimum is also a desirable goal. With these facts, control law design proceeded as described in the next section.

3. Control Law design

a. Approximate method

Specific energy is a function of spacecraft radius. For that reason, specific energy is a very useful parameter that can be used to maintain the satellite within the specified bandwidth. The energy lost when the satellite's radius decreases, is dependent upon the path taken by the satellite in its descent as illustrated in Figure 2 below (exaggerated for clarity).

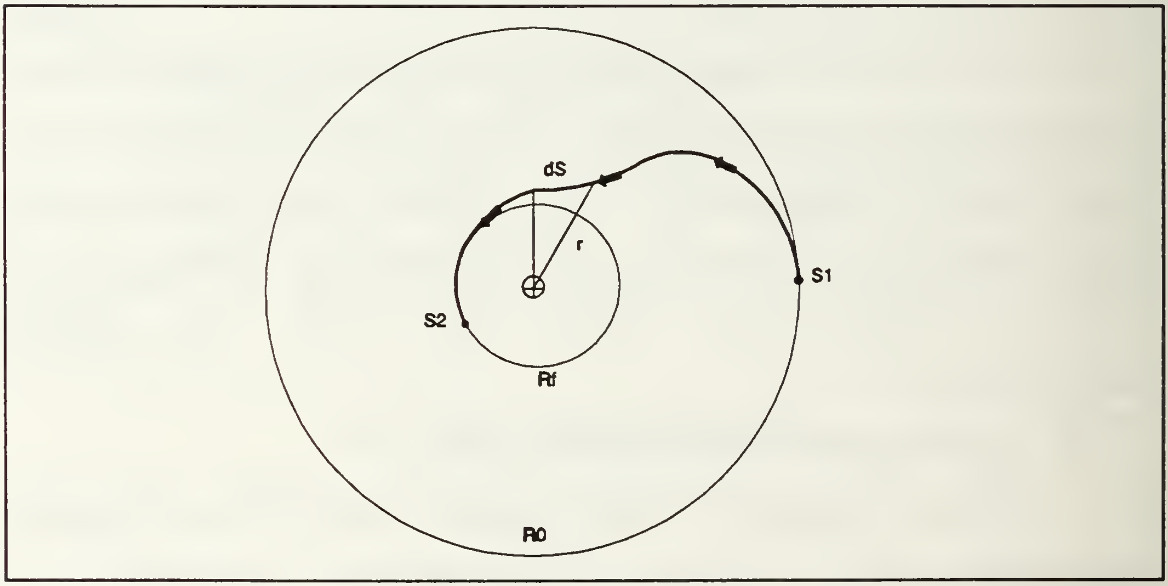

Figure 2 Path Travelled By A Spacecraft Between Two Orbits

If S represents the path travelled by the spacecraft, then S_1 is its initial position and S_2 its final position. The force acting against spacecraft motion is drag, which directly opposes the velocity vector. With this in mind, the energy loss is given by

$$\Delta E = \int_{S_1}^{S_2} D\, dS \tag{21}$$

The arc length S is a function of radius and angle turned through, and is given by

$$S = r\theta \tag{22}$$

Differentiating the above equation yields

$$dS = r d\theta + \theta dr \tag{23}$$

Substituting Equation (23) into Equation (21) yields energy loss in terms of the known variables, r and θ

$$\Delta E = \int_{R_0}^{R_f} D\theta dr + \int_{0}^{\theta} D r d\theta \tag{24}$$

Employing Simpson's rule, the loss in energy can be approximated fairly closely. Assuming atmospheric density, flight path angle, thrust angle and thrust are all constant, Simpson's rule applied over ten iterations yields the energy lost in moving from R_0 to R_f

$$\Delta E = \left(\frac{R_f - R_0}{30}\right) D\theta (30) + \frac{\theta}{30} D r (29) \tag{25}$$

Referring to Figure 2, R_f is the point at which the thrusters will fire. In terms of the control law, R_f is the control variable and can be relabelled as ΔR since it is variable and determines the width of band in which the satellite is maintained. As developed for this model, ΔR is the initial radius R_0 minus one kilometer. This value is chosen so as to maintain maximum orbital deviation within ± 1.5 kilometers of R_0. Now that the energy loss has been approximated, the objective is to determine the length of time to fire the thrusters in order to replace the energy. The return path of the spacecraft is a function of the thrust.

$$\Delta E = \int (\vec{T} - \vec{D}) \bullet d\vec{s} \tag{26}$$

Recognizing that $d\underline{s}$ is related to the time rate of change of the position vector or arc length $\underline{S}$, Equation (26) becomes

$$\Delta E = \int (\vec{T} - \vec{D}) \bullet \vec{v}\, dT \tag{27}$$

Reducing Equation (27) to component form yields

$$\Delta E = \int_{t_0}^{t_f} (T_r - D_r)\, v_r dt + \int_{t_0}^{t_f} (T_{tr} - D_{tr})\, v_{tr} dt \tag{28}$$

Integrating and solving for Δt yields the length of time that the thrusters must fire in order to replace the energy lost due to drag.

$$\Delta t = \frac{\Delta E}{(T_r - D_r)\, v_r + (T_{tr} - D_{tr})\, v_{tr}} \tag{29}$$

Examination of Figure 1 reveals that velocity can be written as

$$v = v\sin(\gamma) \tag{30}$$

and

$$v_{tr} = v\cos(\gamma) \tag{31}$$

Figures 1 through 6 of Appendix B illustrate results obtained from this method for thrust angles of 60° and 65°. Examination of plots of thrust versus orbit (Figures 2 and 5) reveal the inadequacy of this model. Thruster firing times are seen to be on the order of orbits rather than fractions of orbits. This is due to two factors, first and most important being that the energy change is calculated from the initial orbit to the point ΔR where the thrusters begin firing. The problem arises from the fact that the satellite is still in a descent at this point and continues to descend until its motion is reversed through the opposing force of the thrusters. As a result, the satellite loses more energy than is replaced. The second problem arises from the inaccuracies inherent in the assumptions required to perform the approximation. While the first problem is easily resolved, the changes in atmospheric density and flight path angle, while very small, are not constant and the resulting errors combine to render this model unsatisfactory. A more accurate method is to calculate the energy loss directly using the variables derived from integrating the equations of motion.

b. Direct method

Using Equation (18), the initial and instantaneous energies may be calculated at any instant during the trajectory of the spacecraft. As before, thrusters will fire when the spacecraft descends below ΔR. The program then calculates the spacecraft's specific energy each time the equations of motion are integrated. Comparing this value to that of the initial circular orbit, the control law commands the thrusters to fire until they are equal. Examination of Figures 1 through 6 of Appendix C reveals that while results are closer to those expected, this method also appears to be inadequate. Thruster firing times (Figures 2 and 5) remain excessively long. Reevaluation of the model suggested that the solution might be a function of the thrust to drag ratio. Increasing thrust to a value of 300 N and then examining results for thrust angles of 60°, 65° and 70° revealed this to be the solution. Results are found in Appendix D. Thrust angles of 65° and 70° maintain radial deviation within the prescribed bandwidth of three kilometers with a trend that indicates they will remain so indefinitely. Thrust plots (Figures 2, 5 and 8) illustrate that the thrusters are firing over a small portion of an orbit instead over a period of many orbits as before. Plots of spacecraft radius versus orbit are included in each appendix to illustrate the success of the control law in maintaining radial deviation within the three kilometer band. Energy plots are also included as corroberating illustrations of the spacecraft's energy level at each point in its trajectory.

V. ANALYSIS AND RESULTS

Analysis of the validated model is performed in four steps. Prior to testing, drag was returned to its true value of 8.3130×10^{-11} kg/m^3 and thrust was set equal to a value of 25 N. This value is determined by multiplying the thrust to drag value of the test model by the drag actually experienced by the satellite. The thrust to drag ratio with the increased density is

$$\frac{300N}{3.956N} = 75.834 \tag{32}$$

With $\rho = 8.313 \times 10^{-11}$ kg/m^3, drag is calculated to be 0.329 N. Multiplying this to the value in Equation (32) yields a thrust of 25 N.

A. USE OF A CONSTANT DENSITY MODEL

Initial testing maintained a constant density while varying thrust angle. The results obtained from these tests are interesting. As illustrated in Appendix E, approximately six and a half orbits are required for the spacecraft's radius to decay to ΔR. Thruster firing places the spacecraft into a slightly elliptical orbit (typically, eccentricities were found to be on the order of 10^{-4}). Examination of energy plots reveal that the energy of the elliptical orbit is very close to that of the initial circular orbit. This results in one large energy change as the spacecraft initially descends from R_0 and is returned, then, subsequent small changes are required once the spacecraft is established in its "elliptical" orbit. A thrust angle of 70° is seen to yield the best results (see Figure 6 of Appendix E). Radial deviation remains just within the specified radial band with a trend that indicates it will do so indefinitely. At angles of less than 70°, radial deviation steadily increases until it exceeds the prescribed limits. An illustration is provided in Appendix E, for a thrust angle of 65°. Thrust angles greater than 70° follow a trend illustrated by Figure 7 of Appendix E (α=75°) until reaching approximately 85°. Above 85°, increasingly larger values of thrust are required to maintain the spacecraft within the prespecified radial band.

B. USE OF AN EXPONENTIAL ATMOSPHERIC MODEL

Use of a constant atmospheric density model permitted the determination of an optimum angle that could be compared with that determined by a more accurate exponential atmospheric density model. Also, realizing that density changes would be small within a three kilometer band, the constant density model divulged a reasonable facsimile of results obtained from the exponential model. As stated previously, more accurate density models exist, for example, the Jacchia Atmospheric Model (J70). The exponential model, however, provides sufficient accuracy for the development and testing done in this thesis. With this in mind, density is now given by

$$\rho = \rho_0 e^{-\beta(r-r_0)} \tag{33}$$

where β is determined to be -2.12×10^{-5} m^{-1} [Ref. 7]. As predicted, the results are nearly identical to those obtained from the constant density model. A thrust angle of 70° maintains the spacecraft within the three kilometer band with the same trends as described in the previous section. Results are illustrated in Appendix F.

1. Comparison with a Forced-Keplarian Model

It is now possible to compare results obtained from this model with that of a spacecraft experiencing forced-Keplarian motion (thrust equal to drag, resulting in a circular motion). Modifications to the program to obtain a model in which thrust is equal to drag are very simple. The drag subroutine calculates drag then sets thrust equal to it. The subroutine containing the thrust control law is removed from the program entirely since thrusters will fire continuously as long as propellant is available. Drag always opposes the velocity vector which, as previously shown, is defined by the flight path angle γ. If the thrust is exactly opposite and equal to the drag force, then the thrust angle α is equal to the flight path angle. Therefore, modifications consisted of setting $\alpha = \gamma$, removing the subroutine containing the thrust control law and setting thrust equal to the drag calculated in the appropriate subroutine. Since the spacecraft is initially in a circular orbit, validation of these modifications is achieved when the spacecraft's orbital parameters remain unchanged over the test period; in this case, 20 orbits.

Finding that the model performed as expected, plots of propellent consumed over the test period are compared with those for the spacecraft experiencing non-Keplarian motion at a thrust angle of 70°. Results are contained in Appendix G. It is clearly seen that orbital maintenance using forced-Keplarian motion is superior to that using non-Keplarian motion.

2. Further Testing

To determine the "robustness" of the model, two additional tests were performed. In the first, thrust was maintained at 25N while specific impulse was varied over the range of 200 sec, valid for chemical reaction engines, to 2000 sec which is valid for electrothermal engines. In the second test, specific impulse is returned to its initial value of 300 sec while thrust is varied over a range extending from 1N to 35N.

a. Constant Thrust, Varied Specific Impulse

Varying specific impulse while holding thrust constant, forces the rate of fuel consumption to change.

Specific impulse is given by given by

$$I_{sp} = \frac{T}{\dot{m}g_0} \tag{34}$$

where I_{sp} is the specific impulse, T is the magnitude of the thrust, g_0 is the gravitational acceleration at sea-level and m is the change in mass.

Clearly, decreasing thrust results in a corresponding decrease in the rate of propellant consumed over a given period of time. This is graphically represented in Appendix G. The absolute quantity of fuel consumed decreases with increasing specific impulse, but the percent difference between the reboost and forced Keplarian methods remain virtually unchanged.

The percent difference is calculated by taking the ratio of the values of propellant mass at a specific time for thrust-equal-drag plots and reboost plots to determine the relative change between them. This provides a truer comparison of the two schemes than does simply comparing the end values of the plots.

The results illustrated in Appendix G indicate that, while playing a significant role in propulsion system optimization, specific impulse is not a function of the method used to perform orbital maintenance and will not affect the particular outcome of one method more than another.

b. Constant Specific Impulse, Varied Thrust

The previous section illustrated the significance played by specific impulse in minimizing fuel expenditure during orbital maneuvers. Obviously, engine "size" plays an equally important role in that process. It is expected that as thruster size increases, fuel expenditure will increase. Appendix H bears this out. While it is theoretically a simple matter to choose the proper specific impulse (bigger is better), this is not the case when choosing thruster size. Examination of the plots in Appendix H reveal that when comparing engines over a certain time span, the end results do not provide a ready solution. Figure 1 is a case in point. Although this case (1N thruster, I_{sp}=300 sec) results in the least amount of fuel expended over the range of thrusts chosen, it is obvious that this is not a wise choice of thruster size. The thruster fires continuously from its initiation until the end of the test period. The thruster is clearly too small. A five newton thruster, i.e., Figure 2, seems to be a viable engine size, although, without more information, it is difficult to determine positively.

Relatively large thrusters burn for shorter periods of time than smaller thrusters to achieve a common result, but each burn expends more fuel. Smaller thrusters, on the other hand, expend less fuel for a given burn time, yet must burn longer to achieve the same results. The fundamental result of this test is that thruster size is a tradeoff variable that is to be used in conjunction with other factors to achieve desired results, such as minimization of thruster burn time during orbital maintenance.

3. Final Tests

Previous sections have shown that within a narrow radial bandwidth, a model using thrust equal to drag is superior to one using fixed thrust-angle reboost techniques. The question arises as to whether these results will remain valid for larger bandwidths.

As described earlier, the control law commands the thrusters to fire when the spacecraft orbit has decayed a certain distance below the reference orbit. Results are examined for cases where the spacecraft is allowed to descend 20 km, 30 km and 40 km below R_0. Thrust is fixed at 300 N while specific impulses vary between 300 sec, 500 sec and 2000 sec. As for the case of a 3 km bandwidth, a thrust angle of 70° maintained the spacecraft within the desired bandwidth and was therefore used for all cases described below. The tests are performed over a period of 100 orbits. In order to reduce computer time, atmospheric density was once again increased to a value of 1×10^{-9} kg/m^3.

a. Case 1: Thrusters Fire 20 km Below R_0

Rather than choosing a specific bandwidth and adjusting the control law to achieve it, the spacecraft's orbit was allowed to decay a certain distance prior to activation of the control thrusters and the resulting bandwidth measured. This provided expediency since the control law determined the bandwidth rather than having to be adjusted to achieve it. The results are the same in either case so no accuracy is lost with this method. The figures in Appendix I illustrate the results of this case.

Allowing the spacecraft's orbit to decay 20 km prior to activation of the control jets provided a radial band of 55 km. Plots of expended propellant mass versus orbit are provided for the three test cases (I_{sp} = 300 sec, 500 sec and 2000 sec). As in previous cases, thrust equal to drag provides a straight line while reboost is actually a series of steps. Each step is a cycle wherein the spacecraft descends 20 km at which time reboost occurs (vertical portion of plot), after deactivation of the thrusters, the spacecraft once again descends to the point where reboost reoccurs. This is indicated by the horizontal portion of the plot since no fuel is being expended during this portion of the trajectory. As before, the reboost maneuver puts the spacecraft into a slightly eccentric orbit (on the order of 10^{-4}). This accounts for the periodic motion and high number of thruster firings indicated by the mass plots in Figures 2 through 4. As expected, increasing specific impulse reduces the amount of propellant expended over the test cycle.

b. Case 2: Thrusters Fire 30 km Below R_0

Requiring the control law to fire 30 km below the reference orbit provides a radial band of 78 km. Figure 5 is an illustration of spacecraft radius over time. Because ΔR is so large, the reboost maneuver must occur twice before the spacecraft settles into a periodic trajectory that carries it the full width of the radial band. Eccentricity of the osculating orbit, however, remains on the order of 10^{-4}. Once in its periodic trajectory, results are very similar to those of case 1. Figures 6 through 8 illustrate propellant mass consumption over the test period. The first two thruster firings are clearly evident. Once in its periodic trajectory, the mass plots are very similar to those of case 1 and occur for the same reasons.

Comparisons of the mass plots of case 2 to case 1 reveal interesting results. Percent difference comparisons of case 2 to case 1, for identical specific impulses, provides an indication of established trends from which inferences of future results might be made.

We see that for case 1, for each variation of specific impulse, reboosting the spacecraft requires 482 percent more fuel than the use of thrust equal to drag techniques. Case 2 reboost maneuvers require 578 percent more fuel than thrust-cancel-drag maneuvers.

c. *Case 3: Thrusters Fire 40 km Below R_0*

Allowing the spacecraft's orbit to decay 40 km prior to initiating reboost sequences provides a radial band of 100 km in which the satellite trajectory is maintained. Figure 9 illustrates radial deviation of the spacecraft. The increase in ΔR coupled with a fixed thrust requires the satellite to perform three reboost maneuvers before the familiar periodic trajectory is achieved. Thruster firing is clearly evident in the first two incidences, as is the ensuing orbital decay of the resulting (slightly) eccentric trajectories.

Calculating the mass expenditure percentages reveals that reboosting the satellite requires 481 percent more fuel than does setting thrust equal to drag. Although thrust equal to drag is still superior, the difference between the two is decreasing. To further test this result, percentages were calculated for points 43 orbits and 97 orbits into the test period. All values were less than corresponding values calculated in case 2. While these results do not provide conclusive evidence, we may conjecture that a trend is developing, indicating that at some point results from periodic orbital maintenance will equal those from forced Keplarian motion, or as the theory predicts, the plots will reverse and periodic thrusting will become superior.

C. SUMMARY OF RESULTS

Initial testing, utilizing a constant atmospheric density model provided a baseline against which, further testing could be compared. A thrust angle of 70° was found to produce the desired results. Fixing the thrust vector at this angle maintained spacecraft orbital deviation within a three kilometer band nearly indefinitely. Upon determining this angle, the computer program discarded the constant density model and incorporated an exponential atmospheric density model.

This simulation was then compared to a model in which thrust canceled drag. According to the optimal control theory developed in Chapter III, the simulation (reboost model) should prove superior to a thrust-cancel-drag model (relative to the problem of fuel-minimization). In fact, reboost required significantly more propellant to maintain the satellite orbit within the three kilometer band than did thrust equal to drag. To test the robustness of these result, specific impulse was varied between 200 and 2000 sec and thrust was varied between 1 and 35 N. The results remained unchanged. To further test the results, the simulation was tested over much wider radial bands. The results still proved thrust-cancel-drag trajectories superior to reboost models although the difference in efficiency seemed to decrease.

VI. CONCLUSIONS AND RECOMMENDATIONS

As stated previously, optimal control theory states that orbital maintenance using a technique in which thrust cancels drag, is not optimal. This means that some scheme using periodic thrusting must then be optimal. Through the complicated techniques of optimal control theory, a thrust vectoring scheme is shown to indeed be the optimum. If the thrust vector always points along the primer vector, the trajectory is optimal. A sub-optimal scheme using fixed-angle thrusting and parametric variation is presented here as a simplified method of determining the optimality of orbital maintenance.

In each series of tests, minimization of propellent mass using fixed-angle thrusting has proven to be inferior to that in which thrust is set equal to drag. At first glance these results appear to contradict the theory developed by Ross and Melton [Ref. 3]. For small perturbations forced-Keplarian motion proved to be superior to periodic fixed-angle thrusting. As the perturbations increased (indicated by the increasing size of the radial band), it would seem reasonable to expect that the difference in fuel consumption between these two techniques would increase. However, the results of tests described in section A.4 of Chapter V reveal that for large radial bands, the percent difference in propellant mass expended between methods of orbital maintenance using periodic thrusting and forced Keplarian motion, actually appears to decrease. Based on these results, we may conjecture that the percent difference between the two methods tested here will continue to decrease until periodic thrusting yields results superior to those for forced Keplarian motion. Further testing is required before the analytical theory proposed in [Ref. 3] may be conclusively verified.

The problem as presented here is that of fuel-minimization during orbital maintenance. Solving the Mayer optimality problem derived in Ross [Ref. 3] yields the primer vector. This is a very cumbersome method requiring solution of a two-point boundary value problem. If periodic thrusting is done along the primer vector, fuel will be optimized. This thesis has proposed a simpler method using the energy balance of the satellite to achieve similar results. Results, however, indicate that for small perturbations, forced-Keplarian motion will provide the best results.

Ultimately, the goal of this thesis is to provide a method of fuel-minimization that is practical and may be applied to existing systems. Propulsion systems utilizing vectored thrust are highly complex and have a correspondingly higher chance of failure. Additionally, the extreme size of the perturbations required before periodic orbital maintenance would become more economical than forced-Keplarian motion is impractical.

Based on these conclusions, and with the added knowledge that a variable-thrust propulsion system capable of operating continuously over the lifetime of a satellite may also be impractical, it is recommended that further testing of periodic fixed-angle transverse thrusting schemes for small perturbations be accomplished. It is recommended that the Mayer optimality problem described in Ross [Ref. 3] be solved and the primer vector found. The results should then be compared to those described in this thesis to determine the actual amount of savings acquired through optimization. It is possible that the amount of fuel saved may not warrant the cost of building a propulsion system capable of periodic primer thrusting. Additionally, a comparison of orbital maintenance techniques presently in use, with results found in this thesis, should be accomplished to determine their relative efficiency.

APPENDIX A

```
C
C
C     OBJECTIVE: DETERMINATION OF FIXED THRUST ANGLE TO MAINTAIN
C                ORBITAL DEVIATION WITHIN A PREDETERMINED
C                BANDWIDTH.
C
C
C     VARIABLE DEFINITIONS:
C
C                 X(1) = RADIUS (METERS)
C                 X(2) = RADIAL VELOCITY (METERS PER SECOND)
C                 X(3) = THETA  (RADIANS)
C                 X(4) = ANGULAR VELOCITY (RADS PER SECOND)
C                 XDOT(1) = TIME DERIVATIVE OF X(1)
C                 XDOT(2) = TIME DERIVATIVE OF X(2)
C                 XDOT(3) = TIME DERIVATIVE OF X(3)
C                 XDOT(4) = TIME DERIVATIVE OF X(4)
C                 R0 = REFERENCE ORBIT
C                 D = DRAG (N)
C                 E0 = SPECIFIC ENERGY OF REFERENCE ORBIT
C                 E = SPECIFIC ENERGY
C                 MU = GRAVITATIONAL CONSTANT
C                 M = SPACECRAFT MASS (KG)
C                 GAMMAR = FLIGHT PATH ANGLE (RADIANS)
C                 GAMMAD = FLIGHT PATH ANGLE (DEGREES)
C                 TH = THRUST (N)
C                 TMAX = BLOWDOWN (MAXIMUM) THRUST
C                 ALPHAR = THRUST ANGLE (RADIANS)
C                 CD = COEFFICIENT OF DRAG
C                 RHO0 = REFERENCE ATMOSPHERIC DENSITY
C                 RHO = CALCULATED ATMOSPHERIC DENSITY
C                 SPI = SPECIFIC IMPULSE
C                 V = VELOCITY
C                 SREF = REFERENCE SURFACE AREA
C                 G0 = GRAVITATIONAL ACCELERATION
C                 H = INCREMENT OF TIME (STEP SIZE)
C                 PTI = PRINT TIME INTERVAL (STEP SIZE)
C                 T = BEGIN TIME
C                 TF = FINAL (END) TIME
C                 a = SEMI-MAJOR AXIS
```

```
C                 e = ECCENTRICITY
C
C
C     START PROGRAM
          PROGRAM ACTORB
C
C
C     VARIABLE DECLARATION
          IMPLICIT REAL*8(A-H,L-Z)
          DIMENSION X(4),XDOT(4)
C
C
C     DEFINITION OF CONSTANTS
          PI=3.14159265359D+0
          G0=9.806D+0
          T1=0D+0
          N=4
C
CCCCCCCCCCCCCCCCCCCCCCCCCCCCCCCCCCCCCCCCCCCCCCCCCCCCCCCCCCCCCCCCCC
C     MAIN PROGRAM
C
      OPEN(10,FILE='INIT',STATUS='OLD')
      OPEN(11,FILE='OUT',STATUS='NEW')
      OPEN(12,FILE='ORBEL',STATUS='NEW')
      OPEN(13,FILE='RAT',STATUS='NEW')
C
      READ(10,1)R0,V0,M,TMAX,T,TF,H,PTI,CD,MU,RHO0,SREF,SPI
1     FORMAT(13(/,21X,D13.7))
C
C
      PRINT*,'ENTER ALPHA'
      READ*,DEG
      ALPHAR=DEG*PI/180.0D+0
C
C
      INDEX=0
      KOUNT=1
      X(1)=R0
      X(2)=0D+0
      X(3)=0D+0
      X(4)=1.1673449D-3
      E0=M*((V0*V0)/2-MU/R0)
C
C
      WRITE(11,*),'   TIME  ORBITS   RADIUS  VELOCITY  ALPHA
     *ANGLM          ENERGY      TMAX'
      WRITE(11,*),'   (sec)           (km)   (km/sec)  (deg)
     *'
      WRITE(12,*),'     T        a        e     APOGEE    PERIGEE
     *PERIOD '
      WRITE(13,*),'   TIME   ORBITS      DRAG        TH
     *         MASS         GAMMA'
C
C
C     CALCULATIONS
C
C
100   CALL DRAG(SREF,CD,X,R0,RHO0,D,T,V)
      CALL ONOFF(R0,X,TMAX,SPI,G0,TH,E0,GAMMAR,ALPHAR,V,D)
      CALL DIFFEQ(X,XDOT,MU,D,M,TMAX,ALPHAR,T,TH)
      CALL RK4(T,X,XDOT,N,H,INDEX,T)
C
C
      IF (INDEX .NE. 0) GO TO 100
C
C
C     UNIT CONVERSIONS
C
      R=X(1)/1000
      SPEED=(((X(2)*X(2))+(X(1)*X(4))**2)**0.5)/1000
      V=SPEED*1000
      M=M-((TH*H)/(SPI*G0))
      MASS=20000-M
      GAMMAR=ATAN(X(2)/(X(1)*X(4)))
      GAMMAD=GAMMAR*180.0D+0/PI
      ANGM=(X(1)*V*COS(GAMMAR))
      ALPHA=ALPHAR*180.0D+0/PI
      ENERGY=((V*V)/2)-(MU/X(1))
      ORBITS=T/5382.458
C
C
      CALL ORBDAT(ENERGY,ANGM,PI,a,e,APOGEE,PERIGE,PERIOD)
C
C
C     OUTPUT
C
      IF (KOUNT  .LT. DNINT(PTI/H)) GO TO 200
C
      WRITE(11,2)T,ORBITS,R,SPEED,ALPHA,ANGM,ENERGY,TH
      WRITE(12,3)T,a,e,APOGEE,PERIGE,PERIOD
      WRITE(13,4)T,ORBITS,D,TH,MASS,GAMMAD
C
2     FORMAT(2X,F7.0,1X,F5.2,3X,F8.3,2X,F6.4,1X,F6.1,2X,
     *F14.2,2X,F12.2,2X,F5.0)
3     FORMAT(2X,F7.0,1X,F10.3,2X,F4.3,1X,F10.3,1X,F10.3,2X,F10.2)
4     FORMAT(2X,F7.0,2X,F5.2,2X,F12.9,1X,F5.0,1X,F15.3,1X,F10.4)
C
C
```

```
      KOUNT=0
200   KOUNT=KOUNT+1
      IF (TF .GE. T) GO TO 100
C
C
      END
C
C
CCCCCCCCCCCCCCCCCCCCCCCCCCCCCCCCCCCCCCCCCCCCCCCCCCCCCCCCCCCCCCCCCCCCCC
C
      SUBROUTINE DRAG(SREF,CD,X,R0,RHO0,D,T,V)
      IMPLICIT REAL*8(A-H,L-Z)
      DIMENSION X(4),XDOT(4)
C
C
      V=((X(2)*X(2))+(X(1)*X(4))**2)**0.5
      BETA=2.12D-05
      RHO=RHO0*EXP(-BETA*(X(1)-R0))
      D=0.5D0*RHO*CD*SREF*V*V
C
C
      RETURN
      END
C
C
CCCCCCCCCCCCCCCCCCCCCCCCCCCCCCCCCCCCCCCCCCCCCCCCCCCCCCCCCCCCCCCCCCCCCC
C
      SUBROUTINE DIFFEQ(X,XDOT,MU,D,M,TMAX,ALPHAR,T,TH)
      IMPLICIT REAL*8(A-H,L-Z)
      DIMENSION X(4),XDOT(4)
C
C
      A=X(1)*X(4)*X(4)
      B=MU/(X(1)*X(1))
      C=(D/M)*(X(2)/(((X(2)*X(2))+(X(1)*X(4))**2)**0.5))
      E=(TH/M)*SIN(ALPHAR)
C
C
      P=2*X(4)*X(2)/X(1)
      Q=(D/(X(1)*M))*((X(1)*X(4))/(((X(2)*X(2))+(X(1)*X(4))**2)**0.5))
      S=(TH/(X(1)*M))*COS(ALPHAR)
C
C
      XDOT(1)=X(2)
      XDOT(2)=A-B-C+E
      XDOT(3)=X(4)
      XDOT(4)=-P-Q+S
C
C
```

```
99    RETURN
      END
C
C
CCCCCCCCCCCCCCCCCCCCCCCCCCCCCCCCCCCCCCCCCCCCCCCCCCCCCCCCCCCCCCCCC
C
      SUBROUTINE RK4(T,X,XDOT,N,H,INDEX)
      IMPLICIT REAL*8(A-H,L-Z)
      INTEGER INDEX,I
      DIMENSION X(4),XDOT(4),SAVED(4),SAVEX(4)
C
C
      INDEX=INDEX+1
      GO TO (1,2,3,4),INDEX
1     DO 10 I=1,N
      SAVEX(I)=X(I)
      SAVED(I)=XDOT(I)
10    X(I)=SAVEX(I)+.5D0*H*XDOT(I)
      T=T+.5D0*H
      RETURN
C
C
2     DO 20 I=1,N
      SAVED(I)=SAVED(I)+2.D0*XDOT(I)
20    X(I)=SAVEX(I)+.5D0*H*XDOT(I)
      RETURN
C
C
3     DO 30 I=1,N
      SAVED(I)=SAVED(I)+2.D0*XDOT(I)
30    X(I)=SAVEX(I)+H*XDOT(I)
      T=T+.5D0*H
      RETURN
C
C
4     DO 40 I=1,N
40    X(I)=SAVEX(I)+H/6.D0*(SAVED(I)+XDOT(I))
      INDEX=0
      RETURN
      END
C
C
CCCCCCCCCCCCCCCCCCCCCCCCCCCCCCCCCCCCCCCCCCCCCCCCCCCCCCCCCCCCCCCCC
C
      SUBROUTINE ORBDAT(ENERGY,ANGM,PI,a,e,APOGEE,PERIGE,PERIOD)
      IMPLICIT REAL*8(A-H,L-Z)
C
C
      e=(1+(2*ENERGY*ANGM*ANGM/(3.98601208133D+14*
     *3.98601208133D+14)))**0.5
      a=(-3.986D+14/(2*ENERGY))/1000
      APOGEE=a*(1+e)
      PERIGE=a*(1-e)
      PERIOD=((2*PI)/(3.986D+05)**0.5)*(a**1.5)
C
C
      RETURN
      END
C
C
CCCCCCCCCCCCCCCCCCCCCCCCCCCCCCCCCCCCCCCCCCCCCCCCCCCCCCCCCCCCCCCCCC
C
      SUBROUTINE ONOFF(R0,X,TMAX,SPI,G0,TH,E0,GAMMAR,ALPHAR,D)
      IMPLICIT REAL*8(A-H,L-Z)
      DIMENSION X(4),XDOT(4)
C
C
      DELTAR=R0-1000
      V=((X(2)*X(2))+(X(1)*X(4))**2)**0.5
      MU=3.986012D+14
      M=20000
      E=M*((V*V)/2-(MU/X(1)))
C
C      PRINT*,'MU=',MU
C      PRINT*,'E0=',E0
C
      IF (TH .EQ. TMAX) GO TO 99
C
                IF (X(1) .LE. DELTAR) THEN
C
                      IF (E .LT. E0) THEN
                              TH=TMAX
                      ELSE
                               TH=0D+0
                      ENDIF
      ELSE
                TH=0D+0
      ENDIF
C
C
99      IF (E .GE. E0) THEN
               TH=0D+0
        ENDIF

C
C
100   RETURN
      END
```

```
C
C
CCCCCCCCCCCCCCCCCCCCCCCCCCCCCCCCCCCCCCCCCCCCCCCCCCCCCCCCCCCCCCCCCCCC
```

APPENDIX B

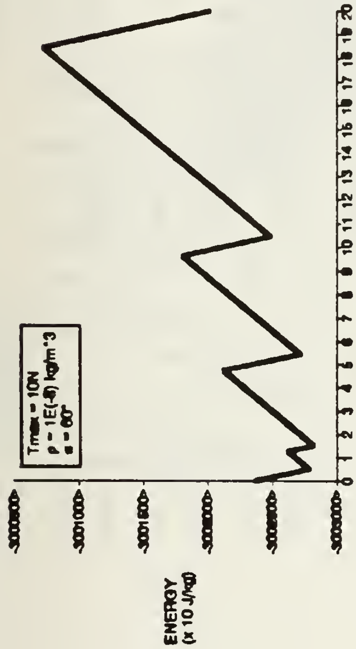

Figure 1

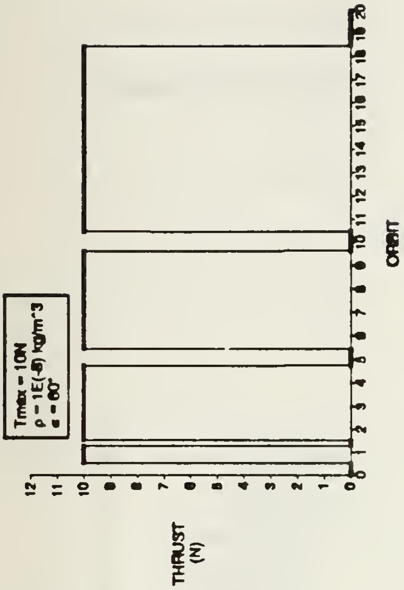

Figure 2

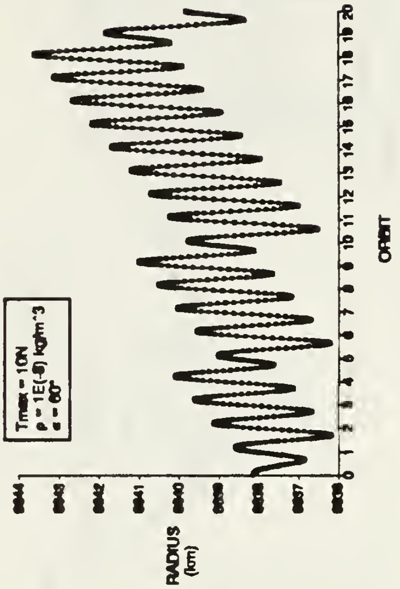

Figure 3

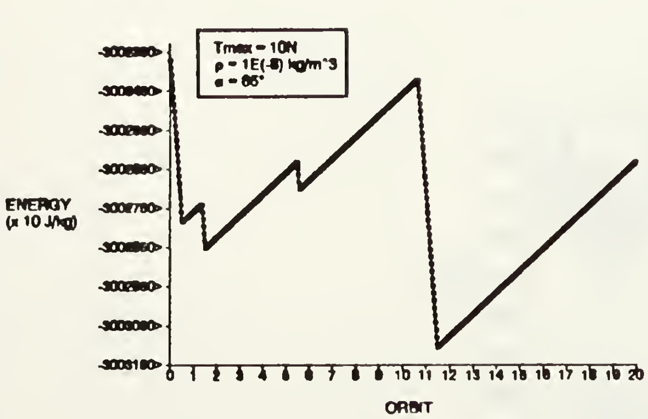

Figure 4

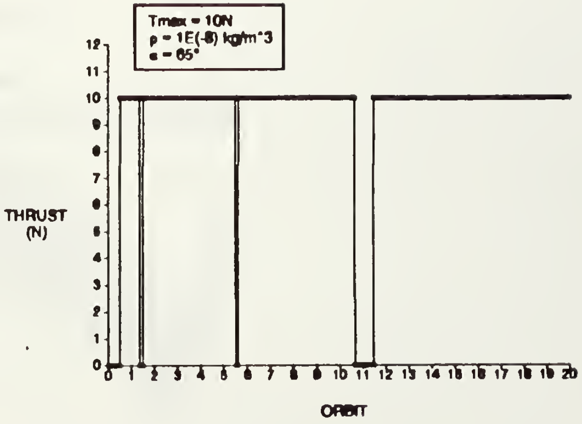

Figure 5

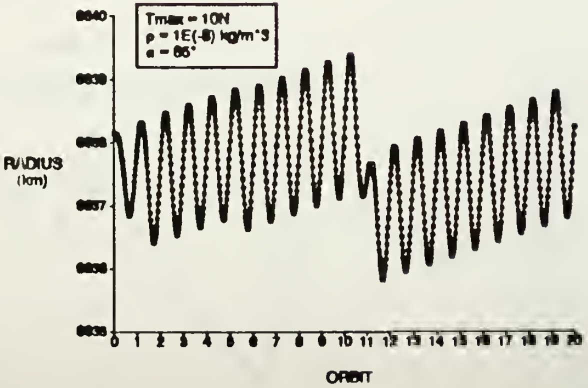

Figure 6

APPENDIX C

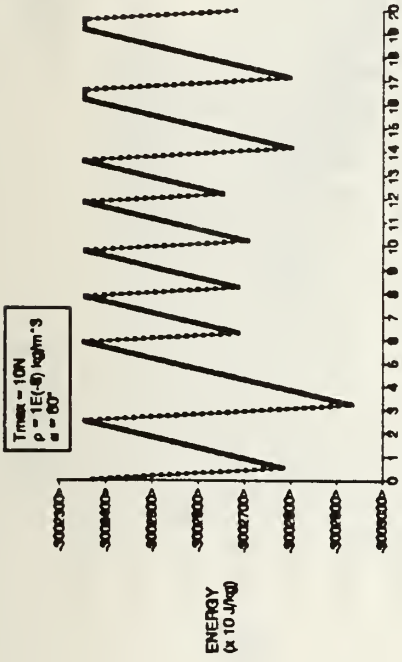

Figure 1

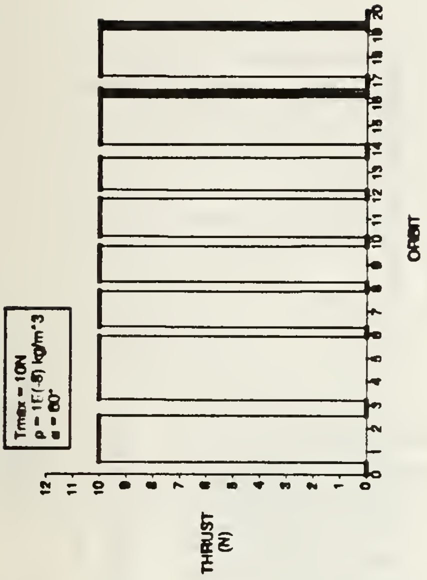

Figure 2

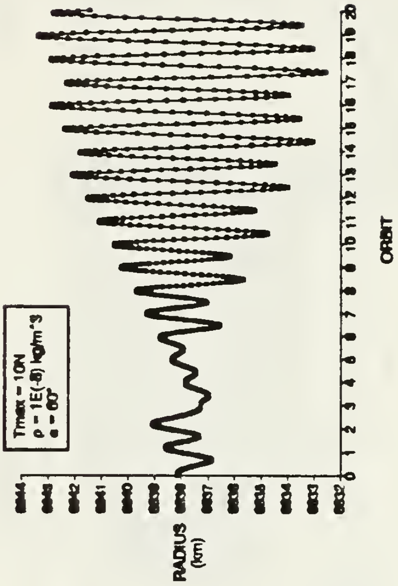

Figure 3

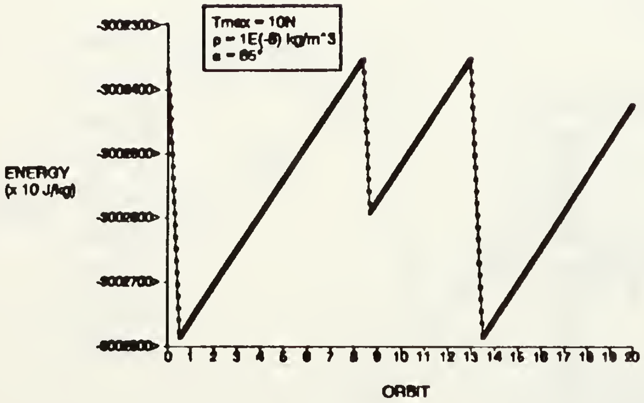

Figure 4

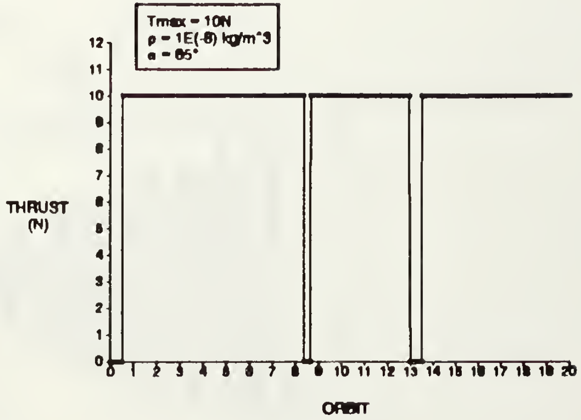

Figure 5

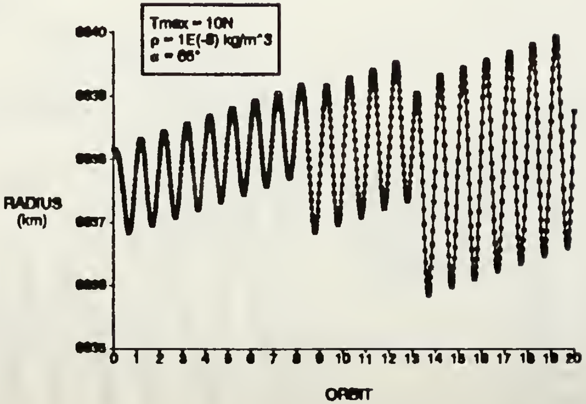

Figure 6

APPENDIX D

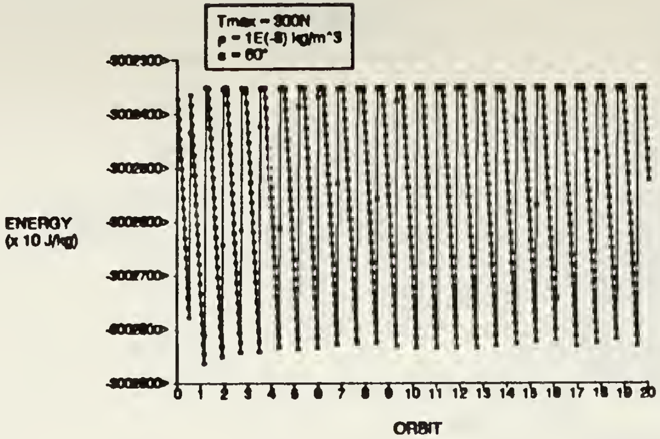

Figure 1

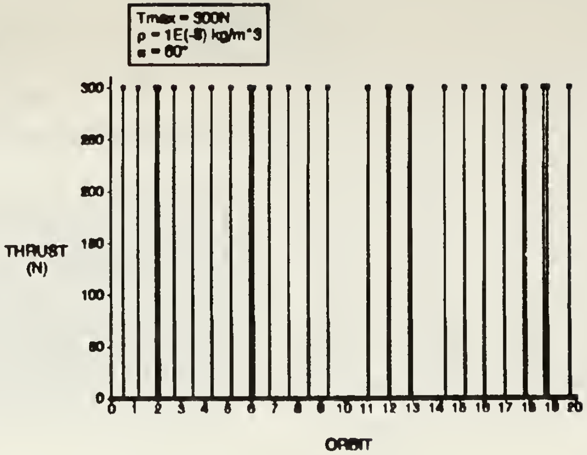

Figure 2

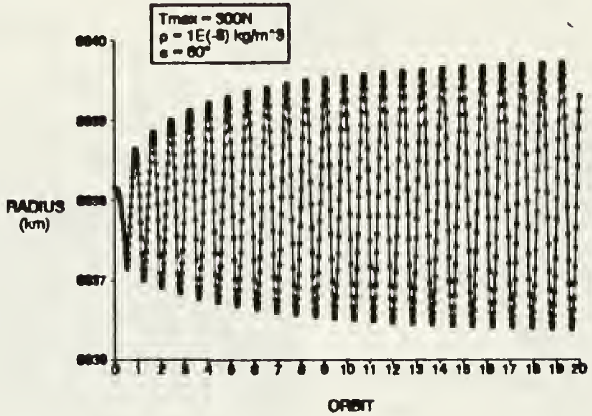

Figure 3

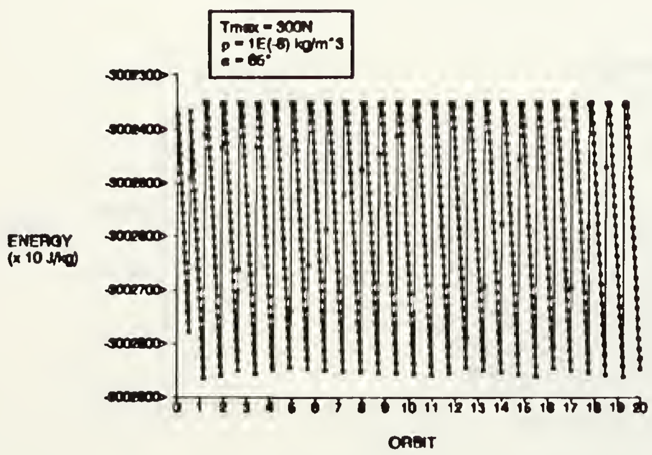

Figure 4

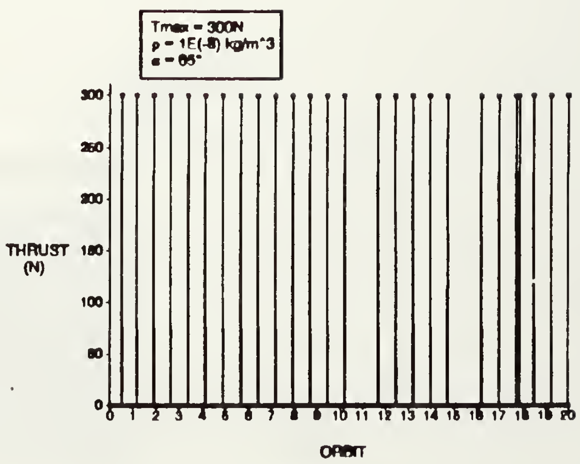

Figure 5

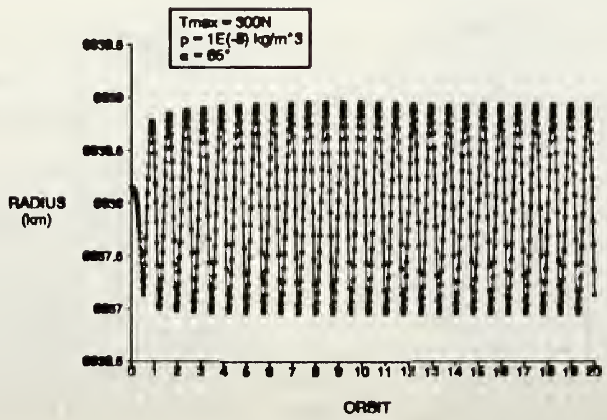

Figure 6

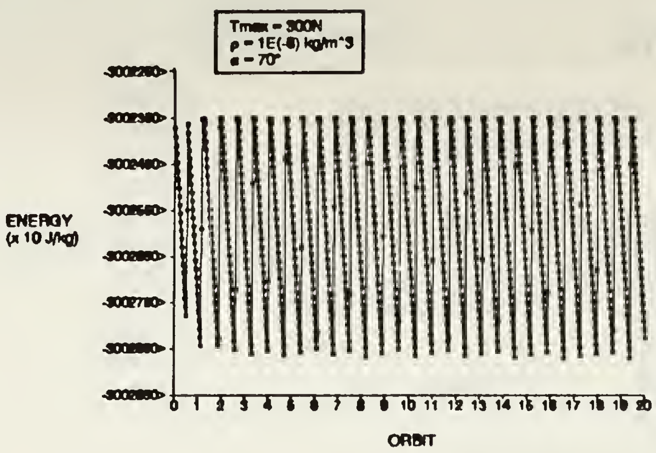

Figure 7

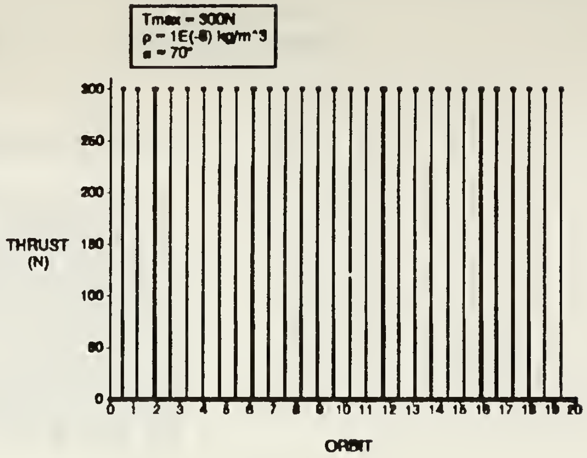

Figure 8

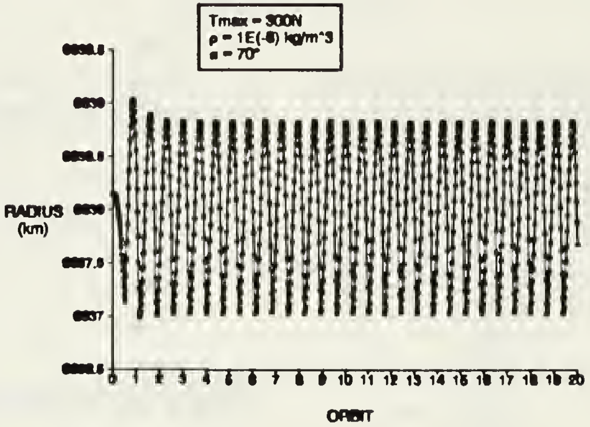

Figure 9

APPENDIX E

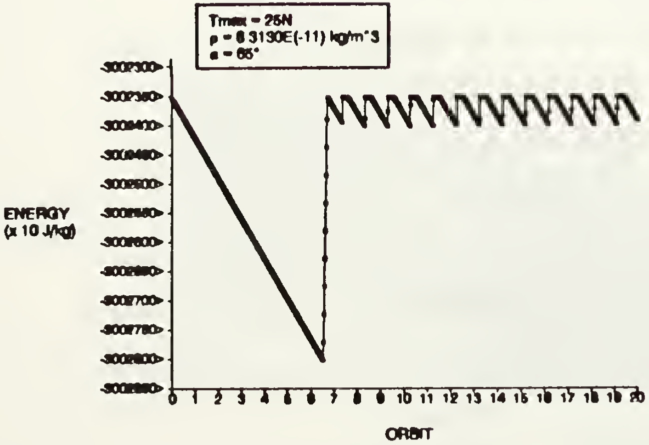

Figure 1

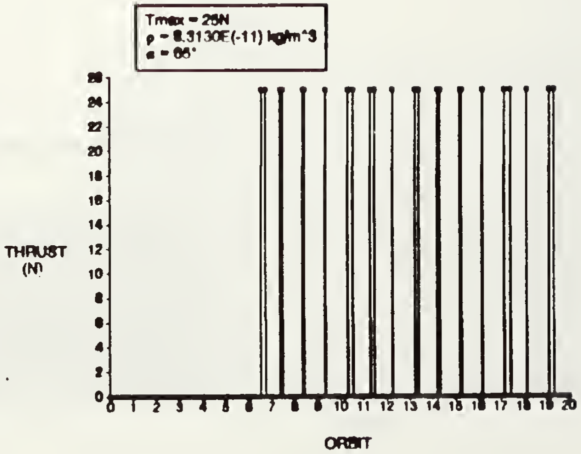

Figure 2

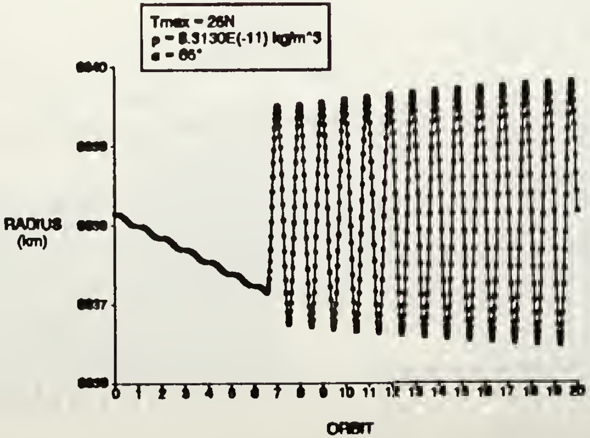

Figure 3

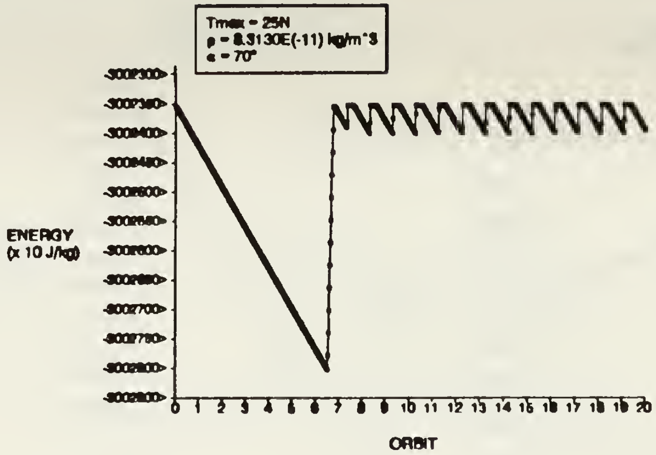

Figure 4

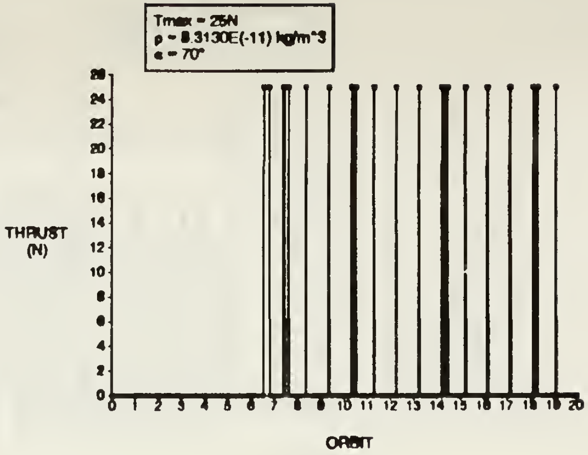

Figure 5

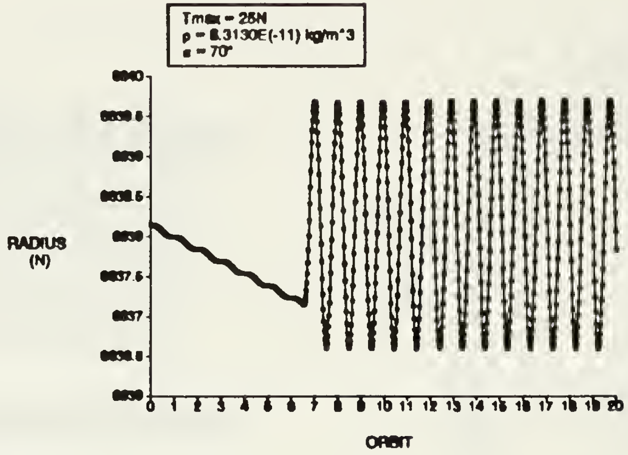

Figure 6

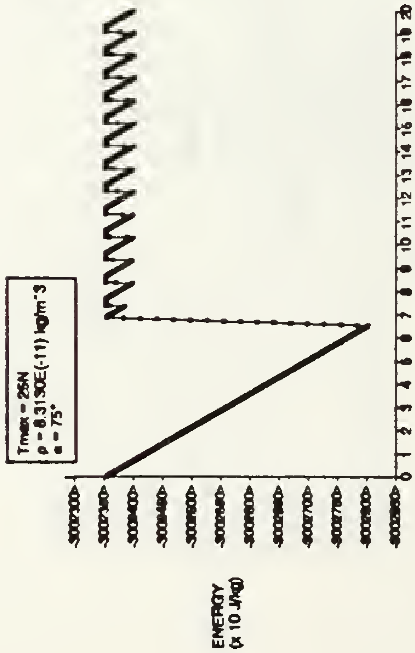

Figure 7

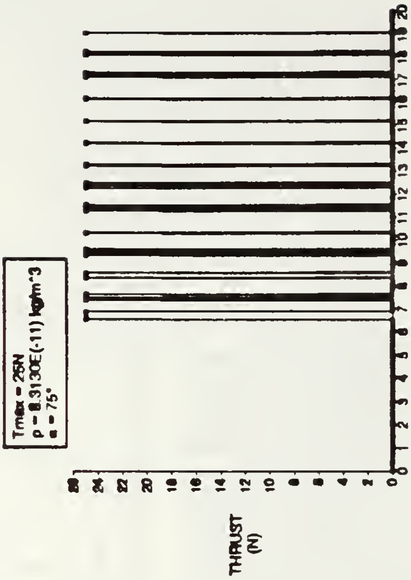

Figure 8

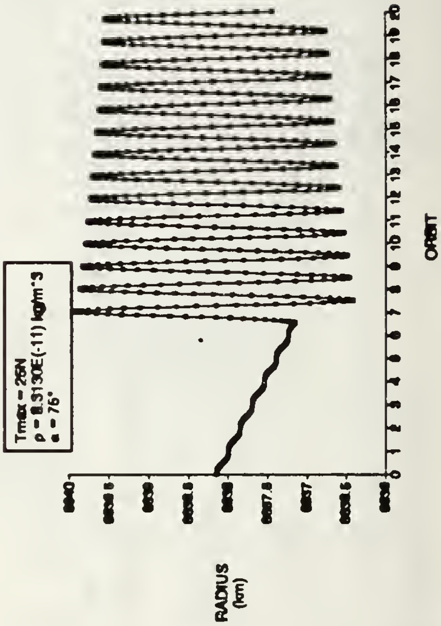

Figure 9

APPENDIX F

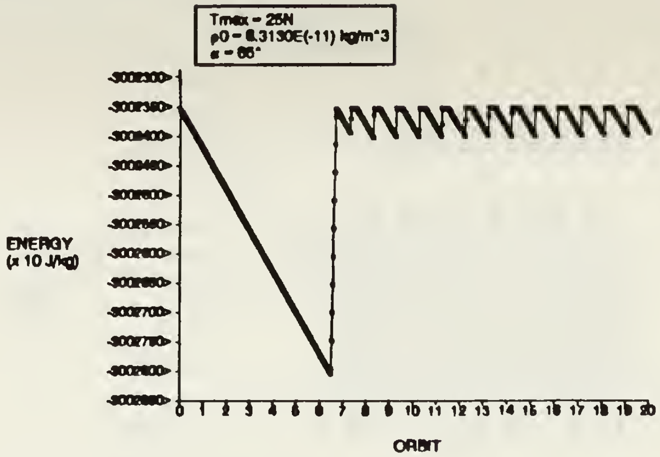

Figure 1

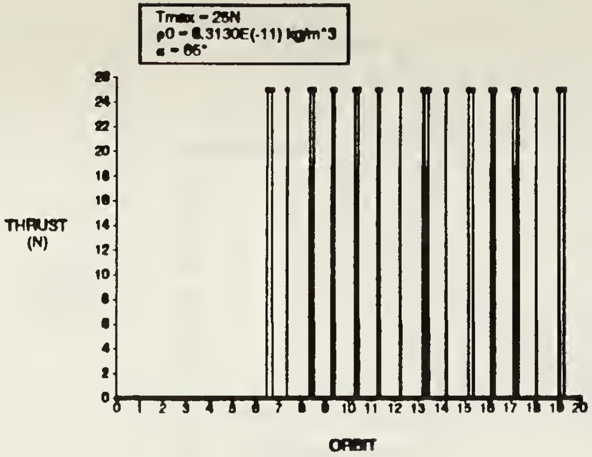

Figure 2

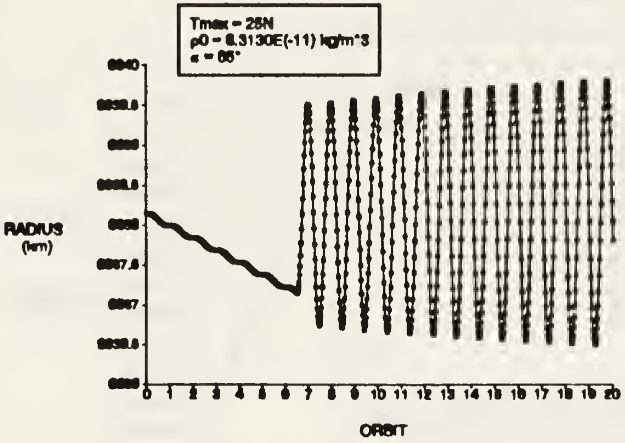

Figure 3

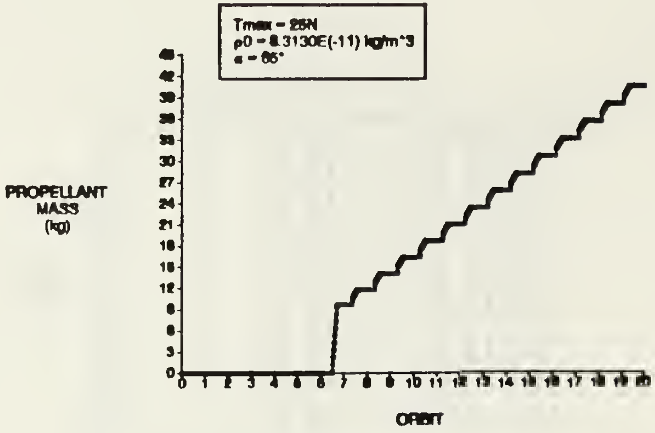

Figure 4

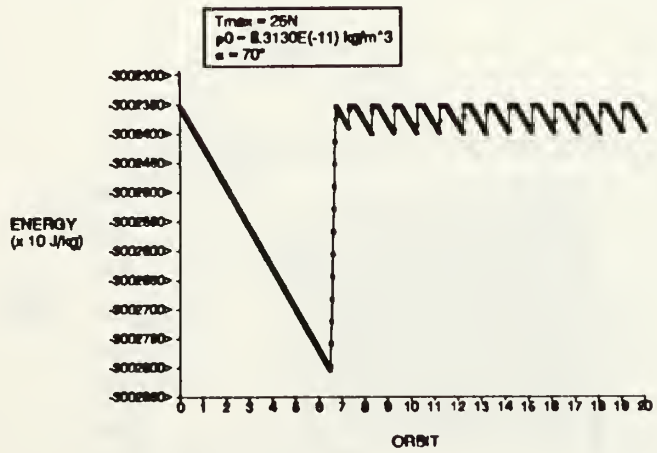

Figure 5

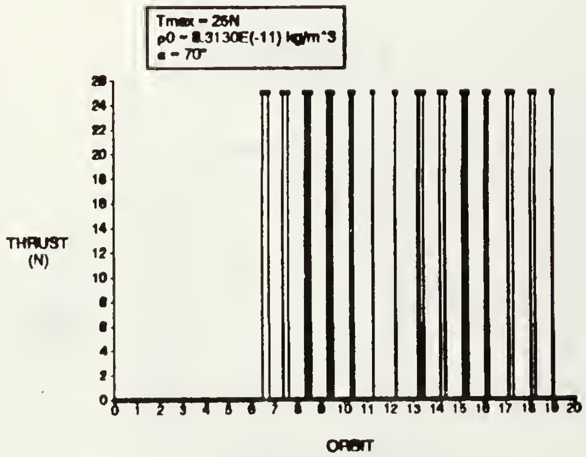

Figure 6

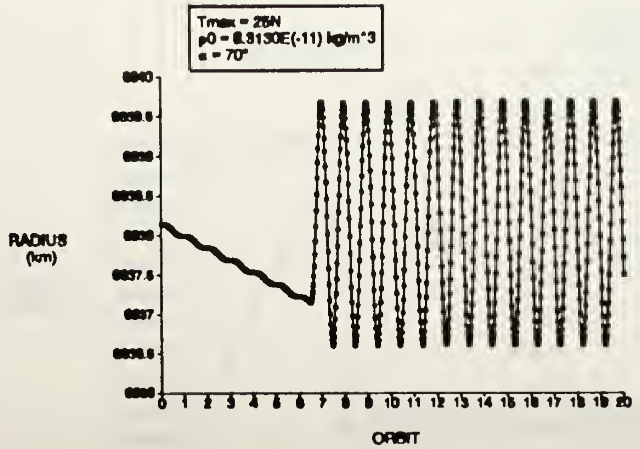

Figure 7

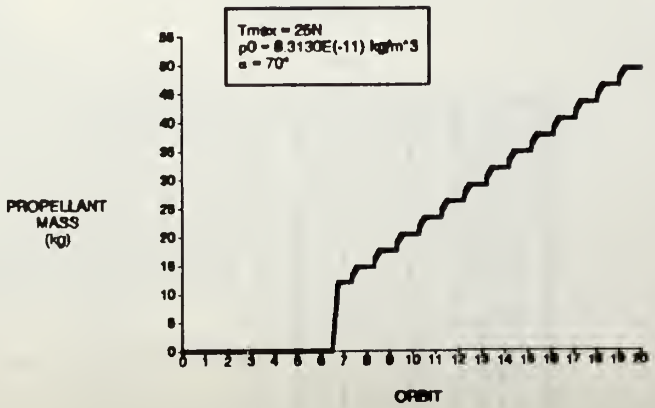

Figure 8

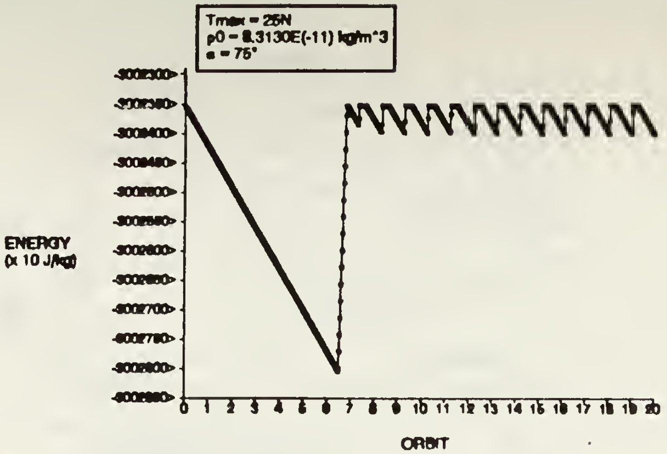

Figure 9

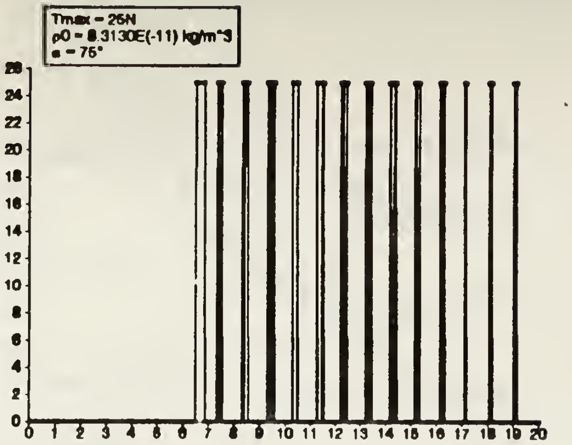

Figure 10

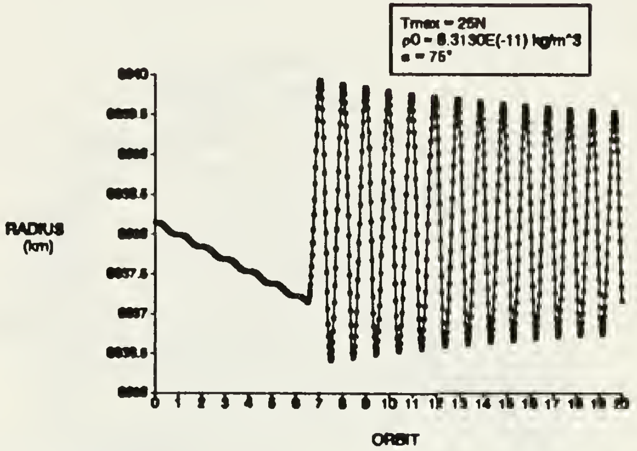

Figure 11

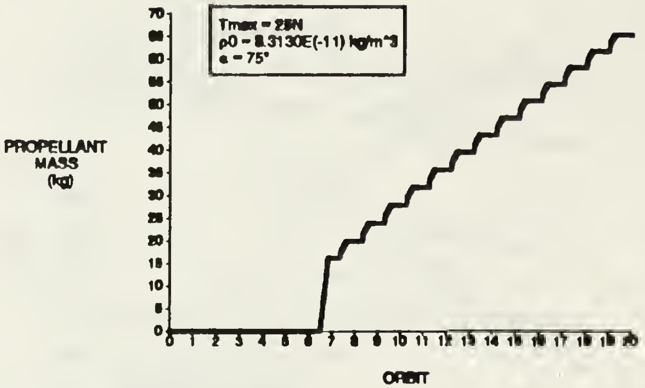

Figure 12

APPENDIX G

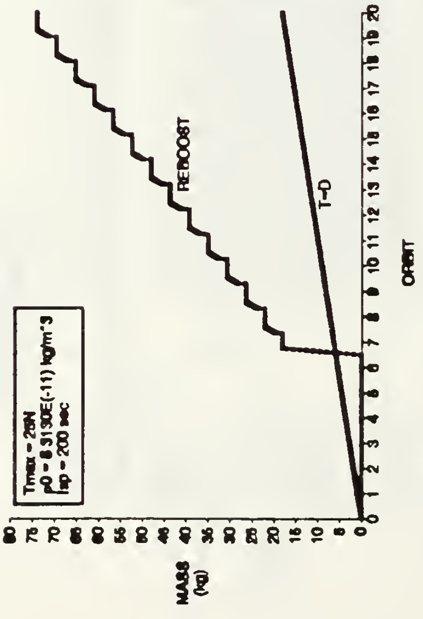

Figure 1

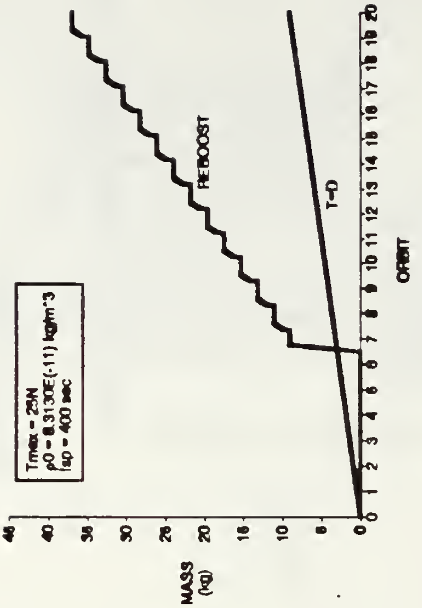

Figure 2

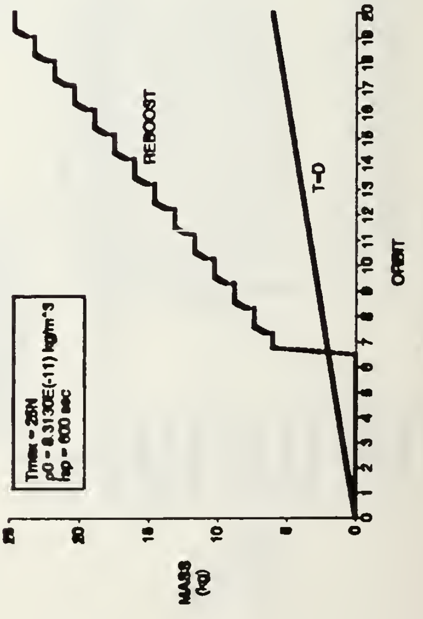

Figure 3

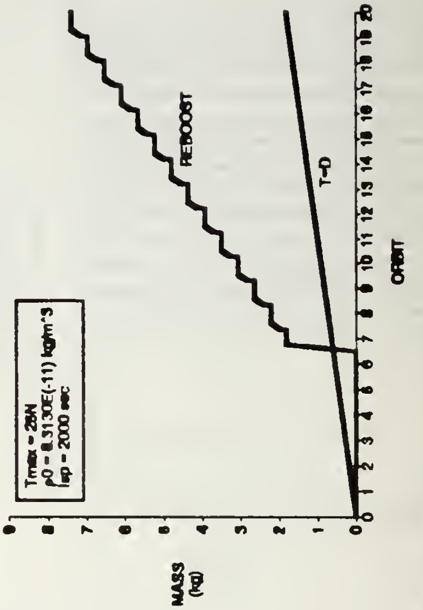

Figure 4

APPENDIX H

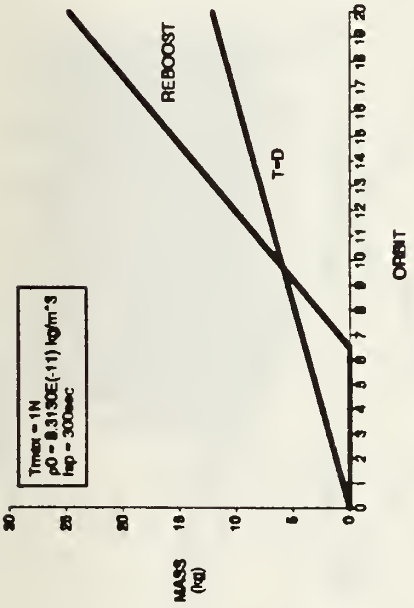

Figure 1

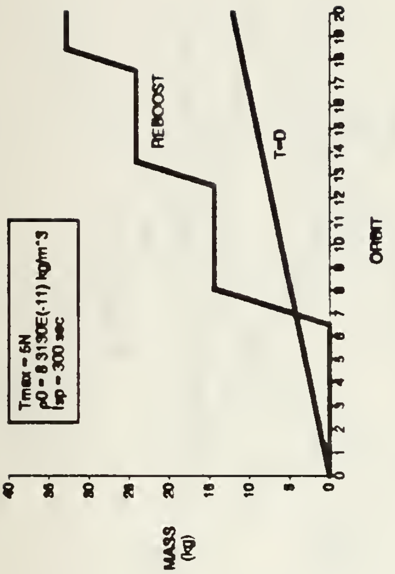

Figure 2

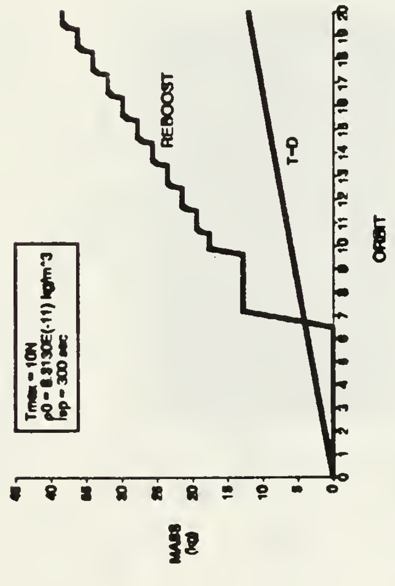

Figure 3

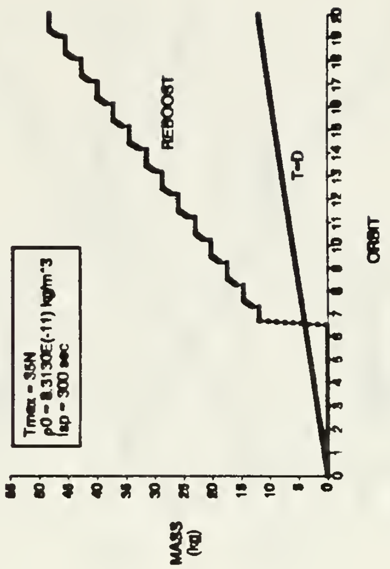

Figure 4

APPENDIX I

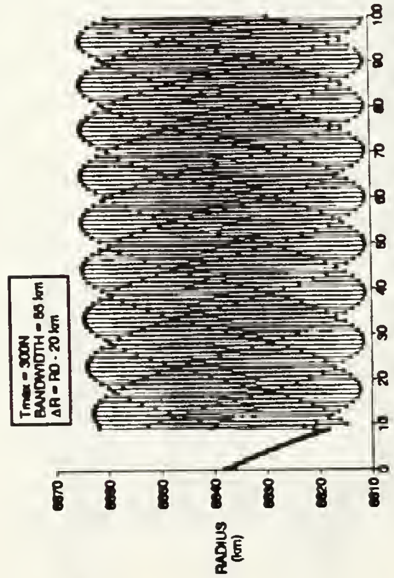

Figure 1

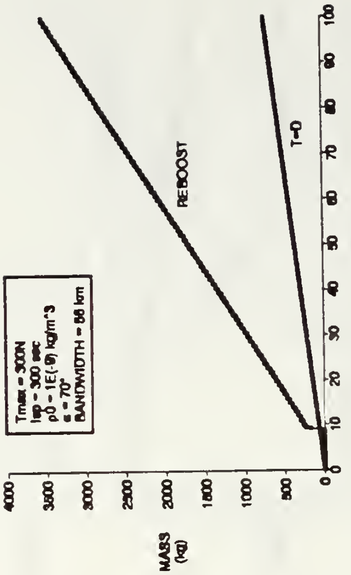

Figure 2

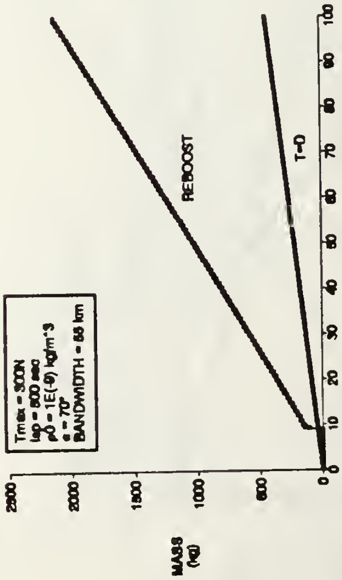

Figure 3

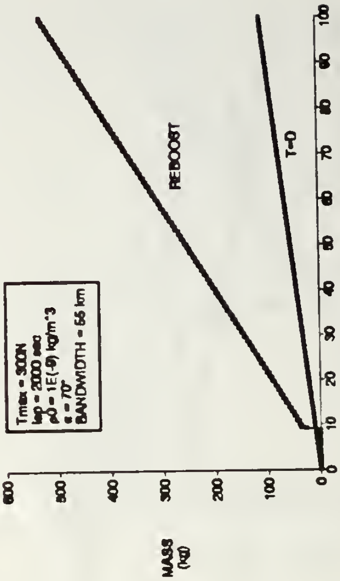

Figure 4

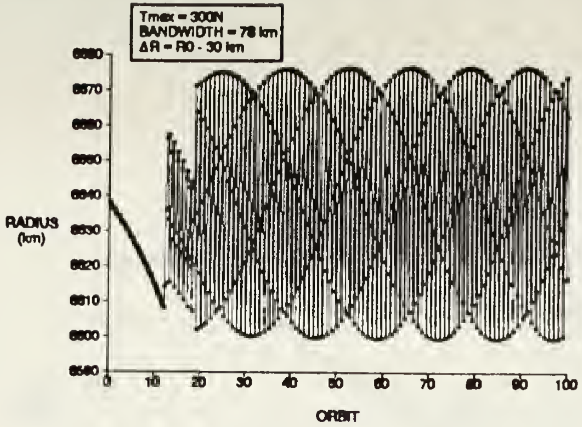

Figure 5

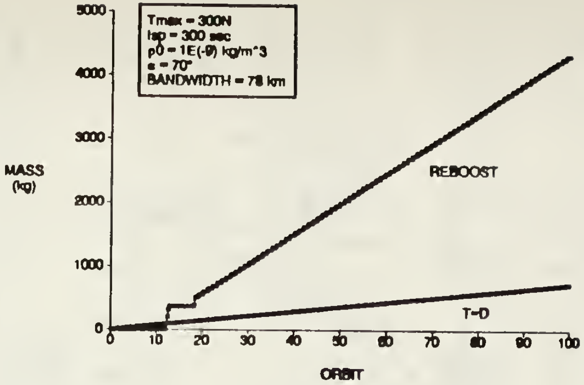

Figure 6

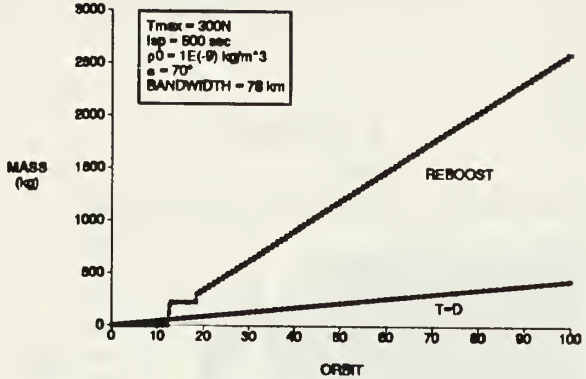

Figure 7

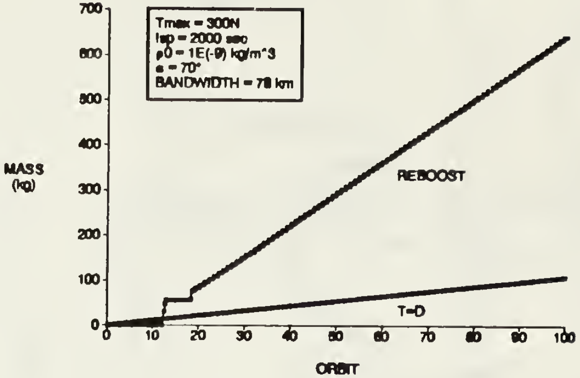

Figure 8

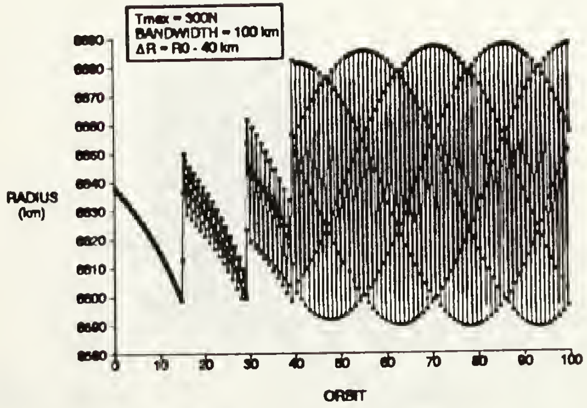

Figure 9

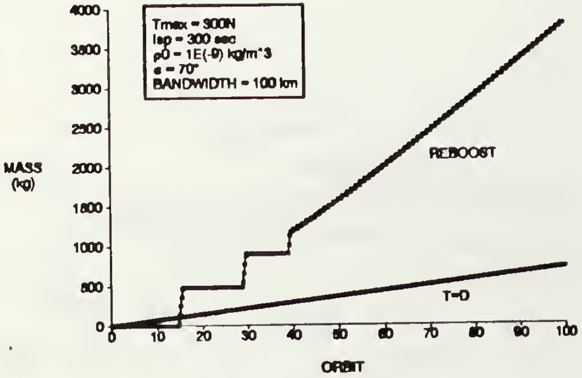

Figure 10

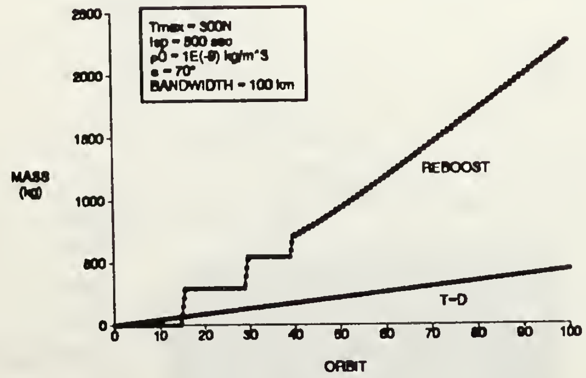

Figure 11

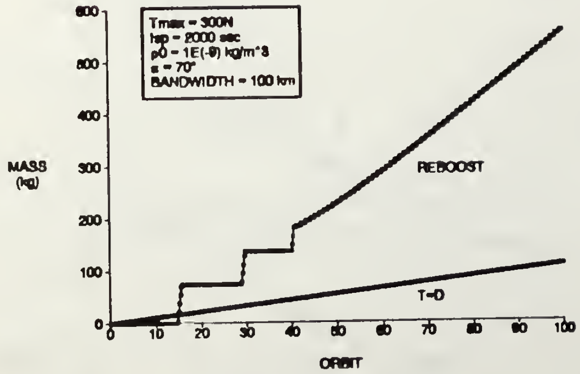

Figure 12

LIST OF REFERENCES

1. Lawden, Derek F., *Optimal Trajectories For Space Navigation*, Butterworths, London, 1963.

2. Marec, J. P., *Optimal Space Trajectories*, Elsevier Scientific Publishing Company, Amsterdam, The Netherlands, 1979.

3. Ross, I. M. and R. G. Melton, *Singular Arcs For Blunt Endoatmospheric Vehicles*, Proceedings of the AIAA/AAS Astrodynamics Conference, Portland, Oregon, August 20-22, 1990, AIAA Paper # 90-2974.

4. Cain, Christina L., *Orbits Containing Arcs of Minimum Altitude Variations*, Masters Thesis, Air Force Institute of Technology, Wright-Patterson Air Force Base, Ohio, June 1989.

5. Eisner, A., *Drag Estimation and Satellite Orbit Determination*, Applied Physics Laboratory, John Hopkins University, March 1980.

6. Kaplan, Marshall H., *Modern Spacecraft Dynamics & Control*, John Wiley & Sons, 1976.

7. *U.S. Standard Atmosphere 1962*, p. 57, United States Government Printing Office, 1962.

INITIAL DISTRIBUTION LIST

		No. of Copies
1.	Defense Technical Information Center Cameron Station Alexandria, VA 22304-6145	2
2.	Library, Code 52 Naval Postgraduate School Monterey, CA 93943-5002	2
3.	I.M. Ross, Code AA/Ro Naval Postgraduate School Monterey, CA 93943-5000	1
4.	David D. Cleary, Code Ph/Cl Naval Postgraduate School Monterey, CA 93943-5000	1
5.	David Pauls VAQ-129 NAS Whidbey Island, WA 98278	1

DUDLEY KNOX LIBRARY
NAVA CHOOL
MONT 101

GAYLORD S

DUDLEY KNOX LIBRARY
3 2768 00307708 2